Bioorganic Chemistry 83 (2019) 111–128

Contents lists available at ScienceDirect

Bioorganic Chemistry

journal homepage: www.elsevier.com/locate/bioorg

Design, synthesis and molecular modeling study of certain VEGFR-2 inhibitors based on thienopyrimidne scaffold as cancer targeting agents

Amna Ghith[a], Khairia M. Youssef[a], Nasser S.M. Ismail[a,*], Khaled A.M. Abouzid[b,*]

[a] Pharmaceutical Chemistry Department, Faculty of Pharmaceutical Sciences and Pharmaceutical Industries, Future University in Egypt, Cairo 12311, Egypt
[b] Pharmaceutical Chemistry Department, Faculty of Pharmacy, Ain Shams University, Cairo 11566, Egypt

ARTICLE INFO

Keywords:
Thieno[2,3-*d*]pyrimidine
Antitumor
VEGFR-2
Kinase inhibitors
Cytotoxic effect
ADMET
Molecular modeling
Cell cycle
Caspase-3 induction

ABSTRACT

Different series of novel thieno [2,3-*d*]pyrimidine derivative (**9a-d,10a-f,l,m** and **15a-m**) were designed, synthesized and evaluated for their ability to *in vitro* inhibit VEGFR-2 enzyme. Also, the cytotoxicity of the final compounds was tested against a panel of 60 different human cancer cell lines by NCI. The VEGFR-2 enzyme inhibitory results revealed that compounds **10d**, **15d** and **15 g** are among the most active inhibitors with IC_{50} values of 2.5, 5.48 and 2.27 μM respectively, while compound **10a** remarkably showed the highest cell growth inhibition with mean growth inhibition (GI) percent of 31.57%. It exhibited broad spectrum anti-proliferative activity against several NCI cell lines specifically on human breast cancer (T7-47D) and renal cancer (A498) cell lines of 85.5% and 77.65% inhibition respectively. To investigate the mechanistic aspects underlying the activity, further biological studies like flow cytometry cell cycle together with caspase-3 colorimetric assays were carried on compound **10a**. Flow cytometric analysis on both MCV-7 and PC-3 cancer cells revealed that it induced cell-cycle arrest in the G0-G1phase and reinforced apoptosis via activation of caspase-3. Furthermore, molecular modeling studies have been carried out to gain further understanding of the binding mode in the active site of VEGFR-2 enzyme and predict pharmacokinetic properties of all the synthesized inhibitors.

1. Introduction

It has become increasingly certain that angiogenesis, new blood vessel formation, plays a central role in the cancer development [1]. Angiogenesis is characterized by the sprouting of capillary blood vessels, a process that is orchestrated by a range of angiogenic factors and inhibitors [2]. The process of new blood-vessel growth has an essential role in development, reproduction and repair. However, pathological angiogenesis occurs not only in tumor formation, but also in a range of non-neoplastic diseases that could be classed together as 'angiogenesis-dependent diseases'. This has important consequences for the clinical use of angiogenesis inhibitors and for drug discovery, not only for optimizing the treatment of cancer, but possibly also for developing therapeutic approaches for various diseases that are otherwise unrelated to each other.

Although proliferating endothelial cells undergoing DNA synthesis are a common hallmark of angiogenic microvascular sprouts, extensive sprouts can grow for periods of time, mainly by the migration of endothelial cells [2]. Angiogenesis does not initiate malignancy but promotes tumor progression and metastasis. Unlike tumor cells, endothelial cells are genomically stable and were therefore originally considered to be ideal therapeutic targets that would not become resistant to anti-angiogenic therapy [3]. For tumors to develop in size and metastatic potential they must make an "angiogenic switch" through perturbing the local balance of proangiogenic and antiangiogenic factors [4].

Comprehensive structural analysis of type I and type II kinase inhibitors has been carried out for various kinds of kinase-ligand complexes. Type I kinase inhibitors, were shown to just bind in and around the region originally occupied by the adenine ring of ATP, hence are typically ATP competitive inhibitors. Type II kinase inhibitors induce the DFG-out (inactive) conformation of the activation loop. This enables them to occupy a hydrophobic site, usually called allosteric site, created by the new rearrangement and directly adjacent to the ATP binding pocket. This allosteric site is only revealed in the inactive conformation of kinase. Furthermore, a bridge portion which is usually an amide or urea moiety generally characterizes type II inhibitors. It forms hydrogen bond (donor-acceptor pair) with the conserved residues in the allosteric site: one hydrogen bond with the side chain of a conserved glutamic acid residue in the α-C-helix and the other with the backbone amide of aspartic acid residue in the DFG motif [5–7].

The Vascular Endothelial Growth Factor Receptor-2 (VEGFR-2) is a class V Receptor Tyrosine Kinase (RTK), expressed primarily in

* Corresponding authors.
E-mail addresses: Nasser.saad@fue.edu.eg (N.S.M. Ismail), khaled.abouzid@pharma.asu.edu.eg (K.A.M. Abouzid).

https://doi.org/10.1016/j.bioorg.2018.10.008
Received 29 July 2018; Received in revised form 21 September 2018; Accepted 4 October 2018
Available online 10 October 2018

endothelial cells, and is activated by the specific binding of Vascular Endothelial Growth Factor (VEGF), secreted by endothelial cells and various tumor cells, to the VEGFR-2 extracellular regulatory domain. Once activated, VEGFR-2 undergoes autophosphorylation, triggering signaling pathways leading to endothelial cell proliferation and subsequent tumor angiogenesis that promotes tumor growth and metastasis [8].

Several small-molecule VEGFR-2 inhibitors have emerged as promising antiangiogenic agents for treatment against a wide variety of cancers and act by competing with adenosine triphosphate (ATP) for the ATP binding site of the VEGFR-2 intracellular kinase domain, thereby preventing the intracellular signaling [9]. Thiophene containing compounds are well known to exhibit various biological effects. Ring systems containing the thienopyrimidine moiety are of interest because of their pivotal pharmacological and biological activities [10]. They bear structural analogy and isoelectronic relation to purine and several substituted thieno[2,3-*d*]pyrimidine derivatives were shown to exhibit prominent and versatile biological activities [11,12]. It is well known that the pyrimidine structure is closely related to three of the four nucleobases uracil, thymine, and cytosine, which fact makes pyrimidines essential building blocks of all living cells [13].

Several inhibitors of VEGFR-2 kinase have been developed as novel anti-cancer therapeutics at low nanomolar concentration including compounds **(I-V)**. A preliminary investigations showed that thieno[2,3-*d*]pyrimidine are as a good mimic as the quinoline, quinazoline and pyrrolo[3,2-*d*]pyrimidine moiety **III**.

With the increase in the number of synthetic inhibitors of VEGFR-2 kinase, it has been important to elucidate the structure activity relationship (SAR) shared among them as shown in Fig. 1.

1. The core structure of most VEGFR-2 kinase inhibitors mentioned above (**I-V**) consists of a flat aromatic or heteroaromatic ring system that binds to the hinge region where the adenine ring of ATP originally binds. It forms an essential hydrogen bond with the backbone NH of Cys 919 linker residue in the enzyme, while the aromatic ring is normally involved in π-π interaction with phenyl ring of Phe 918. Sunitinib (**V**) can form extra hydrogen bond with the amino acid of the hinge region as Glu 917.
2. Extending towards the back pocket of VEGFR-2, the inhibitors pushes through a narrow way lined with the residues Glu885 and Asp1046. The NH motifs of the urea or amide group form two hydrogen bonds with Glu885 residue, whereas the CO motifs form a hydrogen bond with Asp1046 residue [7].
3. Side chain extending toward the solvent-exposed region a feature compromises several chemical structures as methoxy groups as in lenvatinib (**II**) extended aliphatic side chains that are basic in nature as in sunitinib (**IV**), and substituted anilines that are capable of forming hydrogen bond with amino acids of the solvent accessible area. However, sorafinib (**I**) is buried inside the binding pocket without direct interaction with the solvent [15,17–19].
4. Extra aromatic ring system: It is located in the proper position to provide π-π interactions with Phe 1047 as in sorafenib **(I)**, lenvatinib **(II)**.

Features targeting the back allosteric pocket which are resent only in type II inhibitors are responsible for bridging hydrogen-bond network between with CO of N-lobe residue Glu885 and the NH of the activation-loop residue, Asp 1046 involved in the DFG loop move. In the same time, they bear an aromatic ring with hydrophobic substitution that extends to occupy the back hydrophobic pocket. Aryl urea as in sorafenib (**I**), lenvatinib (**II**) are most commonly used to satisfy these requirements. Interestingly, it was reported that lenvatinib (**II**) binds into both the ATP-binding site and a neighboring allosteric region of VEGFR-2 with the DFG motif adopting an 'in' conformation due to its small cyclopropyl group making it an inhibitor that possesses both type I and II binding features [15,17–19].

Analysis of the binding mode of sorafenib **(I)** (PDB code **4ASD**) [20] retained from its X-ray crystal structure in protein data bank (PDB), and

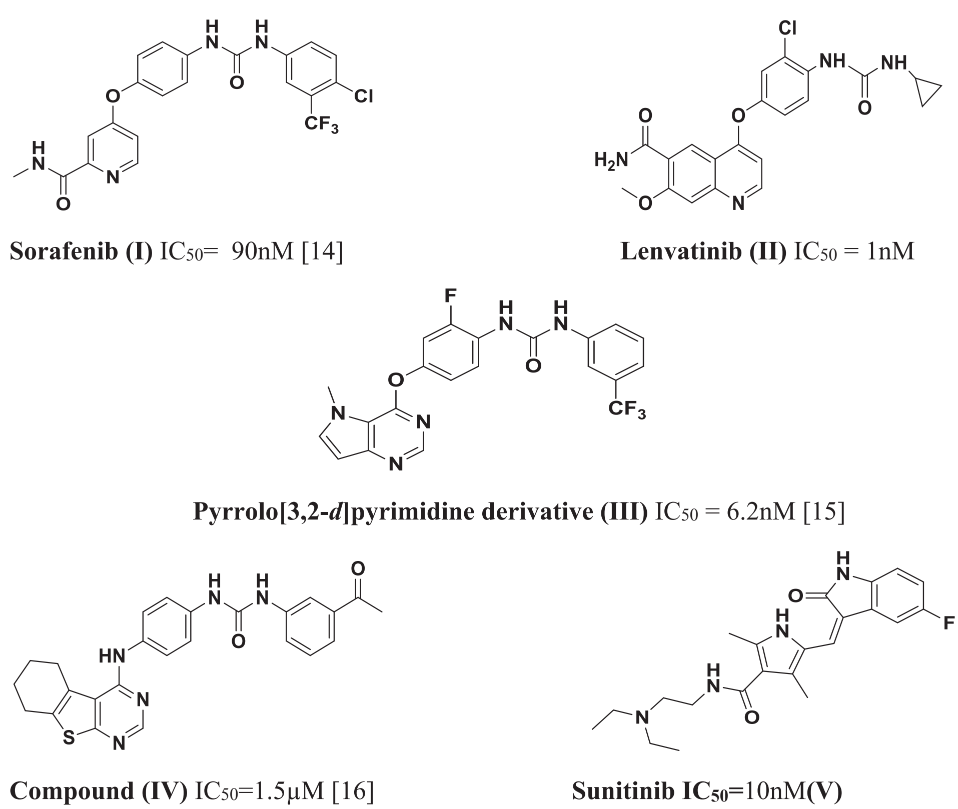

Fig. 1. Chemical structure for clinically approved VEGFR-2 inhibitors **I-V** [14–16].

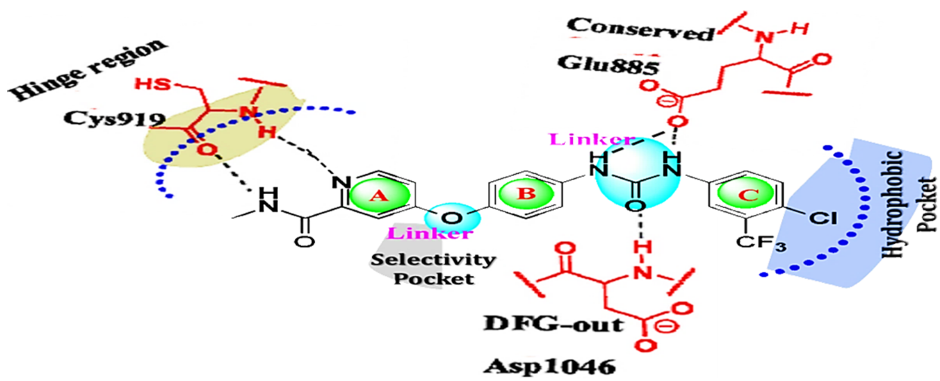

Fig. 2. Pharmacophore model of sorafenib (I) along with catalytic domain of VEGFR-2 kinase.

cyclohexyl thieno[2,3-*d*]pyrimidine derivative (**IV**) [16] (a novel VEGFR-2 inhibitor), bound to VEGFR-2 active site revealed that they form hydrogen bonds with the backbone-NH of Cys919, the side chain carboxylate of Glu885 residue, and backbone-NH of Asp1046 residue. The terminal phenyl moiety occupies the hydrophobic pocket created by rearrangement of the protein as shown in Fig. 2.

Based on comprehensive analysis and extensive study of the reported essential binding features between the VEGFR and reported kinase inhibitors, and as a part of our ongoing efforts to assemble novel small molecules targeting kinases, our strategy was directed towards designing a variety of ligands with promising biological activity.

Herein three series of thieno[2,3-*d*] pyrimidine-based derivatives were designed and synthesized, to act as potential VEGFR-2 type-II kinase inhibitors. Pyrano and pyridino[2,3-*d*] thieno pyrimidine scaffolds were introduced which are not extensively reported as VEGFR inhibitors. The design was based on the bioisosteric modification strategies majorly aiming to improve and enhance the pharmacokinetic properties which are achieved by the introduction of highly polar groups and this was further explored and supported by the ADMET study.

Sorafenib (**I**) and benzothieno[2,3-*d*]pyrimidine derivative (**IV**) [16] (a novel VEGFR-2 inhibitor) were used as lead compounds. The two series were designed bearing the aforementioned essential pharmacophoric fragments for type-II inhibitors, aiming to maintain the same binding interactions between the N-1 nitrogen of the fused pyrimidine scaffolds with the Cys 919 NH in the hinge region, and between the hydrogen bond donor–acceptor pair represented by amide or urea moiety with Glu885 and Asp1046 residues which was preserved in all of the designed ligands.

In addition, two major modifications have been introduced. The first one focused on replacing the pyridine ring of Sorafenib with the thienopyrimidine scaffold also the nonpolar cyclohexyl moiety was replaced by its oxygenated isostere and nitrogen congenere derivatives to give the three series. (**9a-d,10a-f,l,m,14a-m)**. In the second modification the terminal aromatic ring was substituted with various lipophilic groups (R) which are either (electron withdrawing or electron donating) which interact with the terminal allosteric hydrophobic pocket groups this modification was necessarily introduced so we can study their impact on the activity Fig. 3.

2. Results and discussion

2.1. Chemistry

The synthetic pathways adopted for the preparation of the intermediates and that of the target 4-anilino thienopyrimidines compounds are depicted in Schemes 1–3. Final compounds incorporating substituted amide and urea moieties were obtained utilizing the corresponding intermediates (**2a-e, 4a-m**), which were synthesized according to the routes outlined in Schemes 1a and 1b. Synthesis of the intermediates was initiated in Scheme 1a by reacting *p*-nitroaniline with different substituted acid chlorides to give the nitrobenzamide derivatives. The nitro derivatives (**1a-e**) were reduced to their corresponding amines by Pd/C-catalyzed hydrogenation in ethanol to give *N*-(4-aminophenyl)-substituted benzamides (**2a-e**). (Scheme 1a).

Scheme 1a**; Preparation of intermediates 2a-e**

The synthesis of the urea derivatives was achievable using two different methods (**A & B**). Compounds (**4a–g**) were prepared by reacting *p*-nitroaniline with the appropriate isocyanate in dry DCM for 24 h to afford compounds (**3a–g**) [21], which were reduced to their corresponding amino derivatives using 10% Pd-C in methanol [22] to give the 4-aminophenyl substituted phenylureas (**4a-g**) (Scheme 1b). On the other hand, compounds (**4h-m**) were synthesized based on a procedure adopted in method B of Scheme 1b in which, *p*-nitrophenylisocyanate was reacted with different substituted anilines in dry THF for 24 h to give the nitro diaryl urea derivatives (**3h-m**) [23], which were reduced to their corresponding amino derivatives using 10% Pd-C as the catalyst, dissolved in methanol [22] to yield the 4-aminophenyl substituted phenylureas. (**4h-m**) (Scheme 1b).

Scheme 1b **Preparation of intermediates 4a-m**

Finally, the synthesis of the pyranothieno[2,3-*d*]pyrimidine target compounds (Scheme 2) was initiated via the preparation of the key intermediate (**7**), by applying classical Gewald reaction [24] in which, malononitrile, terahydropyran-4-one, and sulfur powder were dissolved in absolute ethanol in morpholine [25] base as a one pot procedure. The 2-aminothiophene derivative was then heated under reflux with DMF-DMA to afford the formamidine intermediate (**8**), which in turn was cyclized directly upon reaction with the different amide and urea intermediates (**2a-d,3a-f,l,m**) in glacial acetic acid to afford the final target compounds (**9a-d, 10a-f, 10l,m**) respectively through Dimorth rearrangement [26].

Scheme 2 **for preparation of pyrano thieno [2,3-*d*] pyrimidine derivatives (9a-d,10a-f,l,m)**

In Scheme 3 similar synthetic procedures were adopted, synthesis of the pyridino thieno pyrimidine based compounds was achieved by dissolving malononitrile, Boc piperidone-4-one and sulphur powder in absolute ethanol and morpholine base as a one pot procedure [25] to give the 2 cyano amino derivative (**12**) which was refluxed with DMF-DMA giving the formamidine derivative (**13**) which enabled the cyclization and incorporation of the 4-anilino urea intermediates (**4a-m**) in a single step in glacial acetic acid through Dimorth rearrangement giving the target compounds [26].

Scheme 3 **for preparation of pyridine Thieno [2,3-d] pyrimidine derivatives (15a-m)**

Spectral data supported the structures of the target 4-anilino pyrano and pyrido thienopyrimidine **(10a-m & 15a-m)** where IR spectra revealed the disappearance of the characteristic nitrile group

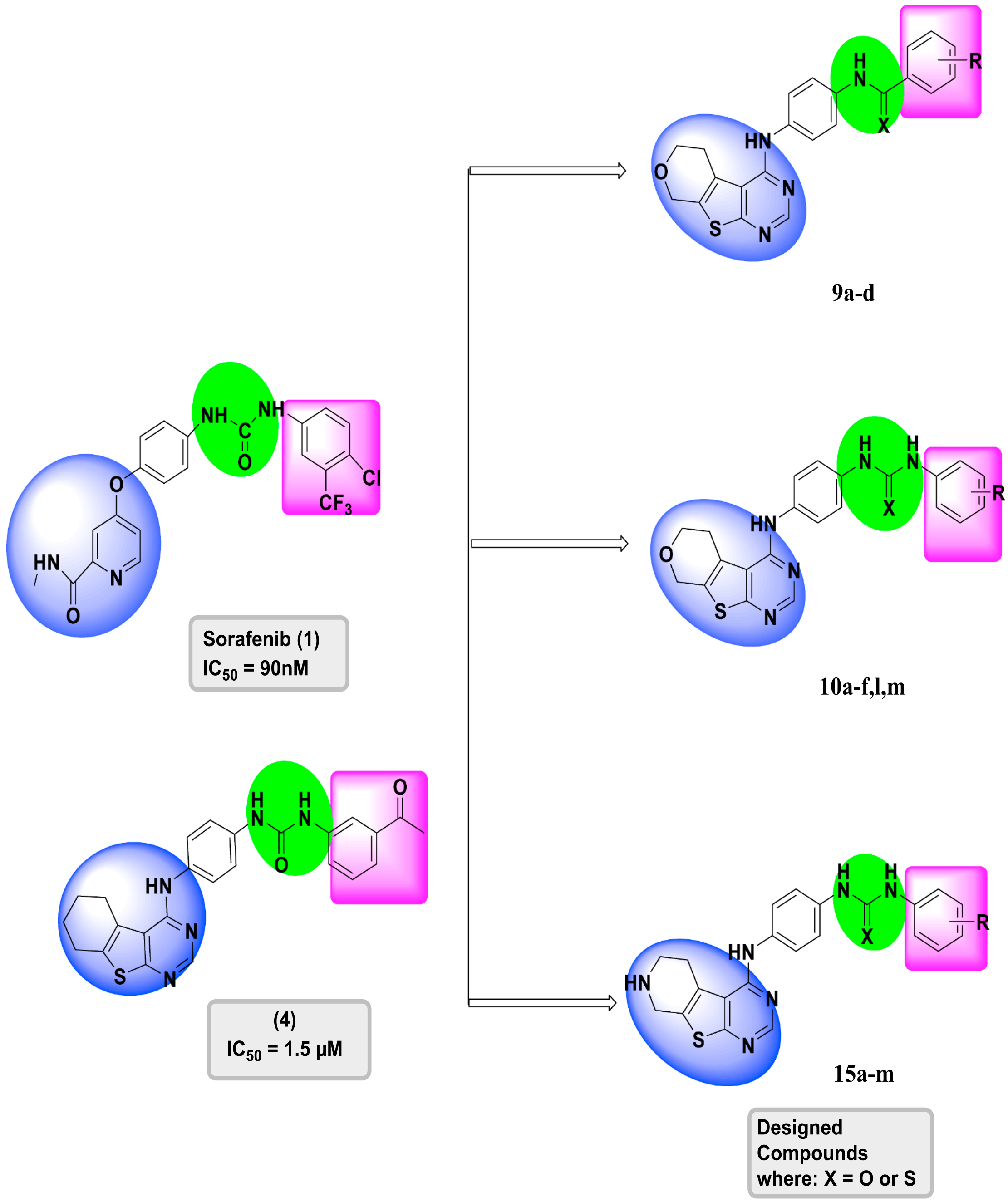

Fig. 3. The essential pharmacophoric features of type II inhibitors aided in the design.

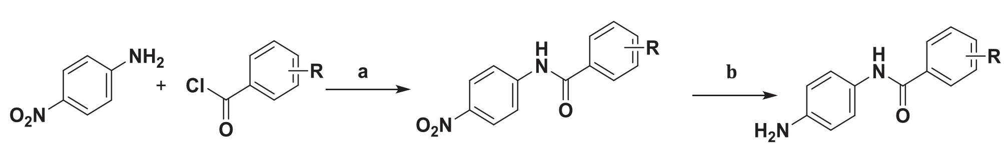

1a-e

2 a -e

1a, 2a, ; R= H
1b, 2b, ; R= 4-Cl
1c , 2c ; R= 4-Br
1d , 2d ; R = 4-OCH_3
1e , 2e ; R = 2-F

Scheme 1a. Reagents and conditions: (a) pyridine stirring rt, 24 h, 70–85% (b) H_2, Pd/C, EtOH, 30 min, 65–85%.

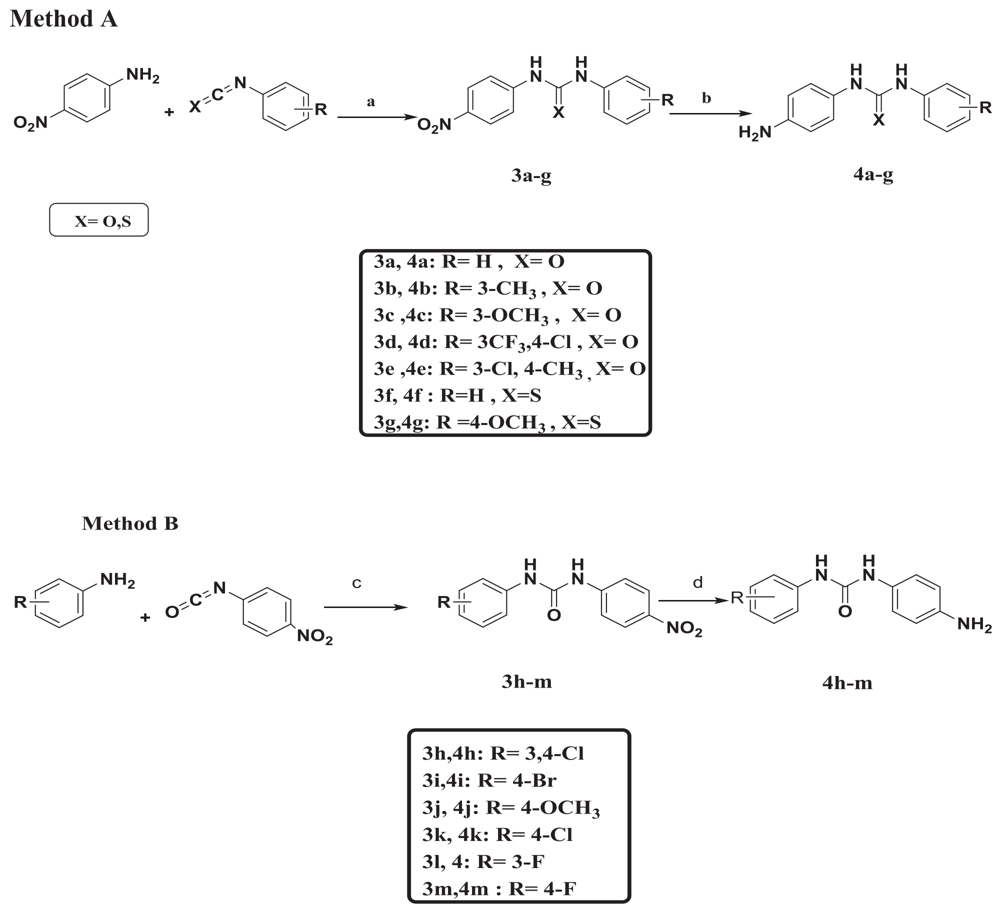

Scheme 1b. Reagents and conditions: (a) DCM, rt, 24 h, 55–85% (b) H_2, Pd/C, MeOH, 30–60 min, 55–80%. (c) THF 60 °C, 24 h, 60–70% (d) H_2, Pd/C, MeOH, 45–60 min, 70–85%.

C≡N signal which was present in the intermediates **(8** and **13)** around 2200 cm^{-1} confirming the cyclization. The appearance of anilino linker N—H peaks was detected between 3100 and 3300 cm^{-1} C—H aliphatic at around 2922 cm^{-1}, C═O amide of the urea moiety appearing around 1685–1690 cm^{-1} and C═N around 1633 cm^{-1}. (**8**). The ^{1}H NMR signals were consistent with protons of the targeted compounds. The spectrum showed three equally integrated signals between δ 9.98–8.50 ppm representing D_2O exchangeable protons of the NH linker and the urea protons all of the synthesized compounds, together with the prominent singlet signal around δ 8.34–8.42 ppm for the CH of the pyrimidine ring in all of the compounds, and all the protons of the introduced aromatic ring system between δ 7.3–8.5 ppm. Also the aliphatic protons were shown as singlet signal at δ 2.28 & 2.02 ppm referring to the extra methyl group in compounds (**10b** & **10e** respectively). Compound (**10c**) showed singlet peak at δ 3.74 ppm corresponding to the methoxy group. ^{13}C NMR of compounds (**10b** & **10c**) showed the peaks corresponding to the aliphatic carbons of the pyran ring at δ 26.62, 64.37, 65.19 ppm in addition to the methyl carbon at δ 21.96 and the methoxy carbon at δ 55.38 ppm respectively.

^{1}H NMR signals revealed singlet signal at δ 1.51 ppm representing nine protons of the tertiary butyl moiety, a singlet signal at δ 4.37 ppm for the two protons at C_7 of pyridine ring, 2 triplet peaks at δ 2.61 ppm and δ 3.61 ppm respectively each corresponding to the two protons of C_4 & C_5 of the pyridine ring. Moreover a singlet signal at δ 4.78 ppm of the exchangeable protons of the amino group was seen.

Moreover, the **^{1}H NMR** showed a new singlet signal at δ 3.19 ppm for six protons of the **—N** $(\underline{CH_3})_2$ group. Another very characteristic singlet peak at δ 7.69 ppm for one proton of **CH═N** group of the side chain was seen.

The synthesized compounds were structurally elucidated by different analytical and spectral data. **^{1}H NMR** signals were consistent with protons of the targeted compounds. The spectra showed a singlet signal around δ 1.5–2.0 ppm representing the nine protons of the *tert* butyl moiety. Two integrated signals ranging from δ 10.07 to δ 8.72 ppm representing D_2O exchangeable protons of the urea protons and NH linker was seen. A prominent signal corresponding to the CH of pyrimidine ring appeared between δ 8.41 and δ 8.34 ppm in all of the compounds, in additional to the protons of the introduced aromatic ring system appearing from δ 6.83 to 8.26 ppm.

Additional aliphatic protons were seen as singlet signal at δ 2.11, and δ 2.45 of the extra methyl group in compounds **(14b&14e)** respectively. Compounds **(14c,14 g,14j)** showed singlet peak around δ 3.72–3.77 ppm corresponding to the methoxy group. **FT-IR** charts revealed stretching signal of N—H group around 3300 cm^{-1}, C—H aliphatic around 2920 cm^{-1}, C═O amide around 1685 cm^{-1}, C═N around 1632 cm.

^{1}H NMR signals were consistent with protons of the targeted compounds. The disappearance of the singlet peak corresponding to the nine protons of the tertiary butyl moiety was very noticeable. Appearance of the additional signal corresponding to the exchangeable D_2O proton of the NH of the pyridine ring in all compounds around δ 10.3–9.72 was seen. Aliphatic protons appeared as singlet peak at δ 2.13, 2.27 of the extra methyl group in compounds **(15b&15e)**. Compound **(15c,15 g,15j)** showed singlet peak at δ 3.78, 3.96, 3.77 ppm respectively corresponding to the methoxy group. **FT-IR** charts revealed stretching signal of N—H group around 3300 cm^{-1}, C—H aliphatic around 2925 cm^{-1}, C═O amide around 1688 cm^{-1} and C═N around 1633 cm^{-1}. The mass analysis of the compounds were consistent.

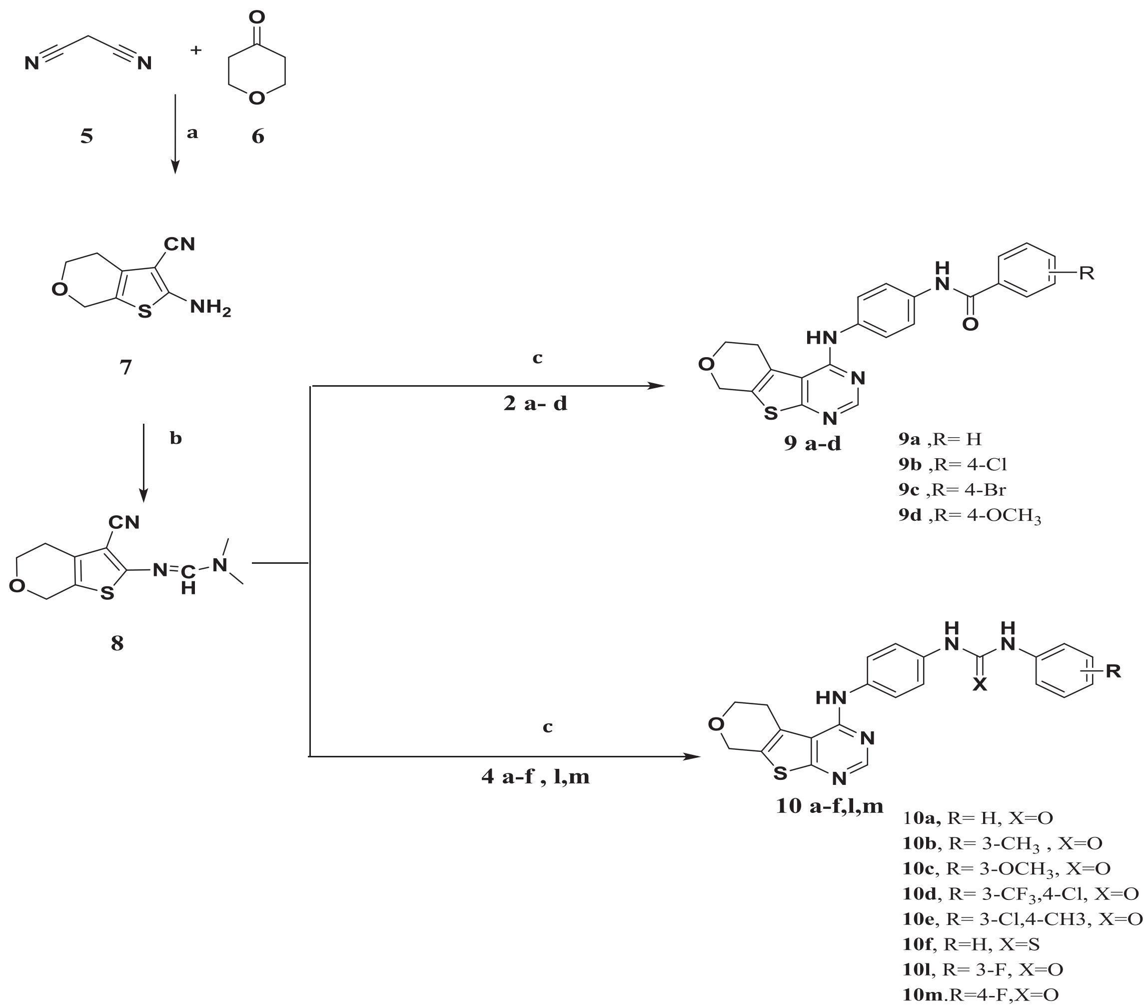

Scheme 2. Reagents and conditions: (a) S, morpholine, W.B at 50–60 °C, 24 h, 66% (b) DMF-DMA, reflux, 5–9 h 69% (c) AcOH, reflux 4–8 h, 30–40%.

3. Biological evaluation

3.1. In vitro VEGFR-2 tyrosine kinase activity

Initial screening at single dose of 10 μM concentration. The VEGFR-2 tyrosine kinase assays were performed at BPS Bioscience, San Diego, CA, USA (www.bpsbioscience.com) using Kinase-Glo Plus luminescence kinase assay kit (Promega). It measures kinase activity by quantitating the amount of ATP remaining in solution following a kinase reaction. The luminescent signal from the assay is correlated with the amount of ATP present and is inversely correlated with the amount of kinase activity The percent inhibition of the tested compounds against VEGFR-2 kinase was compared to reference kinase inhibitor staurosporine at a single concentration of 10 μM. The computer software Graphpad Prism was used for analyzing the luminescence data. The difference between luminescence intensities in the absence of VEGFR (Lu_t) and in the presence of VEGFR (Lu_c) was defined as 100% activity ($Lu_t - Lu_c$). Using luminescence signal (Lu) in the presence of the compound, % activity was calculated as:

% activity = $\{(Lu_t - Lu)/(Lu_t - Lu_c)\} \times 100\%$, where Lu = the luminescence intensity in the presence of the compound. % Inhibition was calculated as: % inhibition = 100 (%) _ % activity.

IC_{50} determination for target compounds against VEGFR-2 was calculated. The values of % activity versus a series of compound concentrations (1 nM–10 nM–100 nM–1 μM–10 μM) were then plotted using non-linear regression analysis of Sigmoidal dose-response curve generated with the equation: $Y = B + (T - B)/1 + 10^{((LogEC50 - X) \times Hill\ Slope)}$, where Y = percent activity, B = minimum percent activity, T = maximum percent activity, X = logarithm of compound and Hill Slope = slope factor or Hill coefficient. The IC_{50} value was determined by the concentration causing a half-maximal percent activity.

In an initial screening; all synthesized final compounds were evaluated for their inhibitory activity against VEGFR-2 kinase at a single dose concentration of 10 μM. At this concentration, the pyrano thieno [2,3-d]pyrimidine derivative (**10d**) and the pyrido thieno[2,3-*d*] pyrimidine derivative (**15d**), both incorporating a substituted biarylurea motif linked via an NH linker to the parent scaffold, have demonstrated a potent inhibition above 80% for the VEGFR-2 kinase activity. Nevertheless, significant inhibition above 70% was also exhibited by several other investigated compounds namely (**10e,15f,15 h,15i**). The mean percent VEGFR-2 inhibition of the investigated compounds bearing both amide or urea moiety at 10 μM concentration are shown in Table 2. (Staurosporine as a reference compound showed 95% VEGFR-2 inhibition) [27].

However, incorporation of different substituents, especially at 3- or 4-position of the terminal phenyl ring was generally well tolerated and resulted in considerable increase in the inhibitory activity. Noticeably, di substitutions in the 3- and 4-positions of the terminal phenyl ring like 3-CF_3, 4-Cl (**10d,15d**) and 3-Cl, 4-CH_3 derivative (**10e,15e**) exhibited the highest inhibition percent ranging from 61 to 85% at 10 μM concentration.

In the pyridothienopyrimidine series compounds incorporating thiourea showed noticeable high inhibitory activity ranging from 78 to

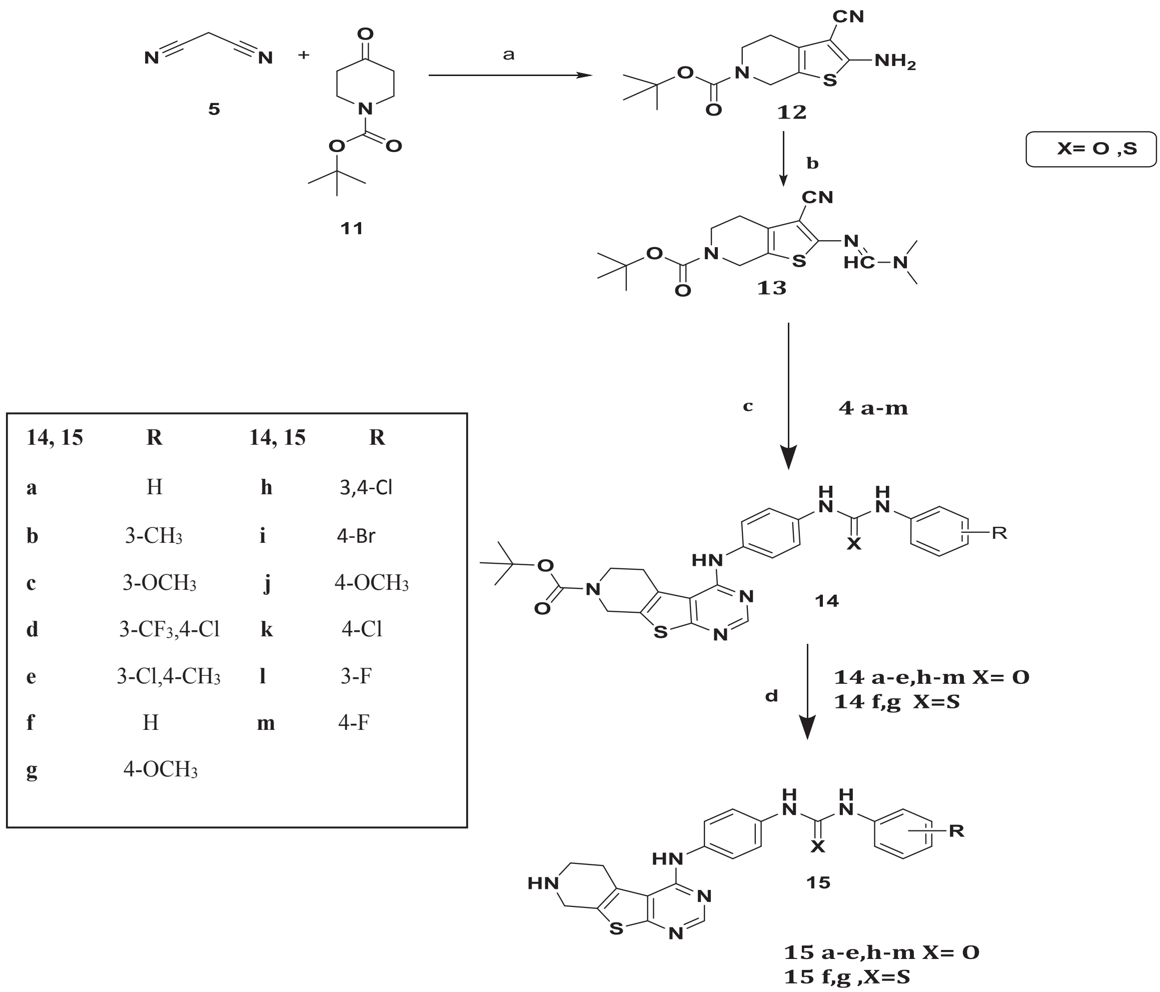

Scheme 3. Reagents and conditions: (a) S_8, morpholine, W.B at 50–60 °C, 24 h, 71.5% (b) DMF-DMA, reflux, 5 h, 67% (c) AcOH, reflux, 10–24 h, (d) 4 M HCl, stirring at 0 °C, 1–3 h, 40–75%.

Table 2
VEGFR-2 inhibition activity results (% inhibition and IC_{50},) of the synthesized compounds.

Cpd ID	Z	X	R	% Inhibition	IC_{50}
10a	O	O	H	19	–
10b	O	O	3-CH_3	7	–
10c	O	O	3-OCH_3	12	–
10d	O	O	3-CF_3, 4-Cl	84	2.5 μM
10e	O	O	3-Cl, 4-CH_3	73	–
10f	O	S	H	12	–
10l	O	O	3-F	15	–
10m	O	O	4-F	8	–
14a	*N*-Boc	O	H	13	–
14d	*N*-Boc	O	3-CF_3, 4-Cl	44	–
14e	*N*-Boc	O	3-Cl, 4-CH_3	8	–
15a	NH	O	H	13	–
15b	NH	O	3-CH_3	44	–
15c	NH	O	3-OCH_3	8	–
15d	NH	O	3CF_3, 4-Cl	85	5.48 μM
15e	NH	O	3-Cl, 4-CH_3	61	–
15f	NH	S	H	78	–
15g	NH	S	4-OCH_3	85	2.27 μM
15h	NH	O	3,4-Cl	76	–
15i	NH	O	4-Br	70	–
15j	NH	O	4-OCH_3	30	–
15k	NH	O	4-Cl	52	–
15l	NH	O	3-F	59	–
15m	NH	O	4-F	58	–

85%. (**15f, g**). Finally it can be concluded that the substitution on the nitrogen of the pyridine ring decreased the enzymatic activity and removal of the tertiary butyl moiety significantly increased the biological activity (**14d&15d**).

Surprisingly, the 3-CH_3, 3-OCH_3, 3F and 4F derivative (**10b,c,l,m**) showed weak inhibition percent 7, 12, 8, 13% respectively. On the other hand, the 4-Br, 4-OCH_3, 4-Cl, 4-F, (15i, 15j, 15 k, 15 l) of the pyridothienopyrimidine series exhibited moderate to good inhibitory activity ranging from 30 to 70% at the same concentration.

Evaluation of potential enzyme inhibitory activity (**IC_{50}**). Promising candidates, which exhibited VEGFR-2 inhibition percent above 80% at 10 μM concentration (**10d, 15d, 15 g**) were further investigated for their dose-related VEGFR-2 enzymatic inhibition at 5 different concentrations (1 nM, 10 nM, 100 nM, 1 μM, 10 μM) to subsequently calculate their IC_{50} values (Table 2). Most of the investigated compounds exhibited potent VEGFR-2 inhibitory activity with IC_{50} values in micromolar range. The pyrano and pyridothieno [2,3-*d*]pyrimidine-based derivatives (**10d, 15d**) linked to the 1-(3-trifluoro-4-chloro phenyl)-3-phenyl urea tail via an NH linkage, showed micromolar VEGFR-2 inhibition (IC_{50} of 2.5 μM, 5.48 μM respectively). While (**15 g**) a pyridothieno[2,3-*d*]pyrimidine linked to 4-methoxy phenyl thiourea tail via an NH linkage showed high inhibitory activity with IC_{50} 2.27 μM.

These data suggest the synthesized compounds display significant VEGFR-2 inhibition.

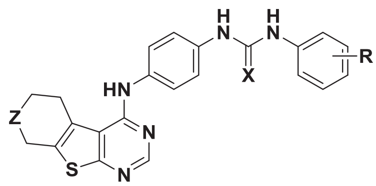

10a-f , l,m,14a,d,e 15a-m

3.2. In vitro antiproliferative activity against NCI 60-cell line

Twenty of the final compounds were selected by the National Cancer Institute "NCI", NIH, Bethesda, Maryland, USA (www.dtp.nci.nih.gov) under the Developmental Therapeutic Program (DTP), namely (10a, 10b, 10c, 10d, 10e, 10f, 14a, 14b, 14c, 14e, 14f, 14g, 14i, 14k, 15a, 15b, 15c, 15e, 15f, 15g). Selection of the screening representing the different chemotypes of this work, was based on the ability of the submitted compounds to add diversity to the NCI small molecule compound collection. The operation of this screen utilizes 60 different human tumor cell lines, classified into nine subpanels namely; leukemia, melanoma, lung, colon, brain, ovary, kidney, prostate and breast cancer, all of the tested compounds were tested at initial single dose 10 μM inhibition percent assay on the full NCI 60 cell panel. The results were expressed as cell percentage growth inhibition (GI%) for each of the tested compound on each of the 60 NCI cell line panel (Table 3 of SM [29–35,37–43,46]).

In light of the NCI-60 results, the following observations could be outlined:

In the thieno[2,3-*d*]pyrimidine series linked to biarylureas, the unsubstituted derivative **10a** remarkably showed the highest cell growth inhibition with mean growth inhibition percent of 31.57% **(SM)**. It exhibited broad spectrum and good anti-proliferative activity against several NCI cell lines, the highest growth inhibition was shown against the breast cancer T7-47D cell line with 85.5% inhibition, also good inhibition was seen on the renal cancer A498 and UO-31 cell lines with 77.65 and 59.81% inhibition respectively, moreover significant inhibition was noticeable on the ovarian cancer IGROV1 and SK-OV-3 cell lines with 64.54% and 65.96% respectively. The leukemic CCRF-CEM, MOLT-4 and SR cancer cell lines with growth inhibition 43.11, 44.08 and 40.08% respectively, the non-small cell lung cancer HOP-62 and-NCI-H522 cell lines with cell growth inhibition 51.34% and 57.08% respectively, the colon cancer HT29 cell line with 54.03% inhibition, the CNS cancer SF-539 and SNB-75 cell lines with growth inhibition 47.59, 54.3% respectively, the melanoma UACC-62 cell line with 42.55% inhibition, and the prostate cancer PC-3 cell line with 42.36%, while **10d** on prostate cancer PC-3 cell line showed inhibition of 39.19% and **10e** on breast cancer BT-549 cell line had 41.54% growth inhibition.

The unsubstituted thiourea derivative **10f** showed moderate inhibitory activity against melanoma UACC-62 cell line with 47.28% while both **10f** and **14f** showed average inhibition on renal cancer UO-31 cell line 41.74, 47.93% respectively. On the other hand both **14b** and **14c** showed growth inhibition on breast cancer T-47D cell line of 51.12 and 41.44% respectively. Moreover 48.95% growth inhibition on renal cancer UO-31 cell line with compound **14b** was observed.

On the other hand the deprotected thieno[2,3-*d*]pyrimidine series linked to biarylureas **15** showed moderate inhibitory activity; **15a** on Melanoma UACC-257 cell line growth inhibition of 43.29%, ovarian cancer SK-OV-3 cell line of 42.66% inhibition. **15b** had growth inhibition on renal cancer UO-31 cell line of 42.12%. **15c** on the non-small lung cancer NCI-H522 cell line with inhibition of 44.59%. The 4-Cl derivative **15d** exhibited inhibition on several cancer lines specifically on ovarian cancer IGROV1, SK-OV-3 cell lines of 44.32 and 46.39% inhibition respectively, renal cancer UO-31cell line with cell growth inhibition 43.58%, breast cancer T-47D cell line with 45.25% inhibition.

On the contrary, compounds (**10b, 10c, 10d, 14a, 14e, 14g, 14i, 15e, 15f, 15g**) showed weak activity against most of the investigated cell lines.

3.3. Flow cytometry cell cycle analysis

Many of the reported anticancer compounds exert their cytotoxic effect by blocking the cell cycle progression or by inducing apoptosis. To gain better understanding of the possible mechanism and mode of action of the synthesized compounds, cell cycle analysis was performed. Compound **10a** was examined for its effect on cell cycle progression on both MCF-7 breast cancer and PC-3 prostate cancer cell lines as it previously exhibited good cytotoxicity on those specific kinds of cell lines. Cell cycle analysis protocol depends upon the quantitation of DNA content using propidium iodide DNA staining. Cells were washed in PBS and fixed for 3 min at 4 °C by adding cold 70% ethanol dropwise during vortex application, which ensured fixation and avoided clumping of cells. Cells were then treated with ribonuclease (50 µl of 100 µg/ml stock) to ensure staining of DNA only, finally (200 µl of 50 µg/ml stock) of propidium iodide was added.

Since sorafenib induces cell cycle arrest to most cancer cells at G0/G1 stage therefore, exploit of the effect of compound **10a** on the cytometric flow on MCF-7 breast cancer and PC-3 prostate cancer cells was interesting to specifically detect at which stage it could induce apoptosis on the aforementioned cell lines. As shown in Fig. 4 the assay outcomes proved that it prompted cell cycle arrest at G0-G1 stage on MCF-7 cell line, when compared to normal control cells, in Dip G0-G1 phase an increase from 43.87% to 47.02% was seen together with an increase from 31.11% to 35.21% at G2-M phase. Meanwhile **10a** made a prominent increase on PC-3 cell line at G0-G1 phase from 41.95 to 62.01%. The above results may suggest that the apoptotic pathway is a possible mechanism for the antitumor activity of the tested compounds.

3.4. Caspase-3 study

Caspase-3 is an enzyme that plays a key role in programmed cell death, or apoptosis. Its referred to as the henchman that goes around and executes the cell. It is activated in every mammalian cell-type provoking to die, considered among the hallmarks of apoptosis. Caspase-3 colorimetric assay was performed as a more sensitive test to examine and discover the potentiality of compound **10a** to induce apoptosis against the two specified MCF-7 and PC-3 cancer cell lines. The following assay protocol was tracked in which; caspase-3 reaction buffer (100 µl) was added to each well in the reaction plate. Then 100 µl of cell lysate was mixed with Caspase-3 reaction buffer spontaneously. Immediate measurement of the absorbance of each sample at 405 nm (initial reading), and final reading was recorded after exactly 30 min. The absorbance obtained from the assay was compared with control normal cells and displayed in Fig. 5. The absorbance increase is directly proportional to the amount of active caspase-3 present in each culture sample.

Compound **10a** showed 10 fold increases in absorbance on both PC-3 cell line and MCF-7 when compared with the control. This reflected its highest ability to activate caspase-3 enzyme and dramatically re-inforce apoptosis of cancer cells. The above results were correlated with the previous cell cycle assay where, the active compound**10a** which boosted 62.01% cell cycle arrest at G0-G1 phase also prompted apoptotic pathway through high activation of caspase-3.

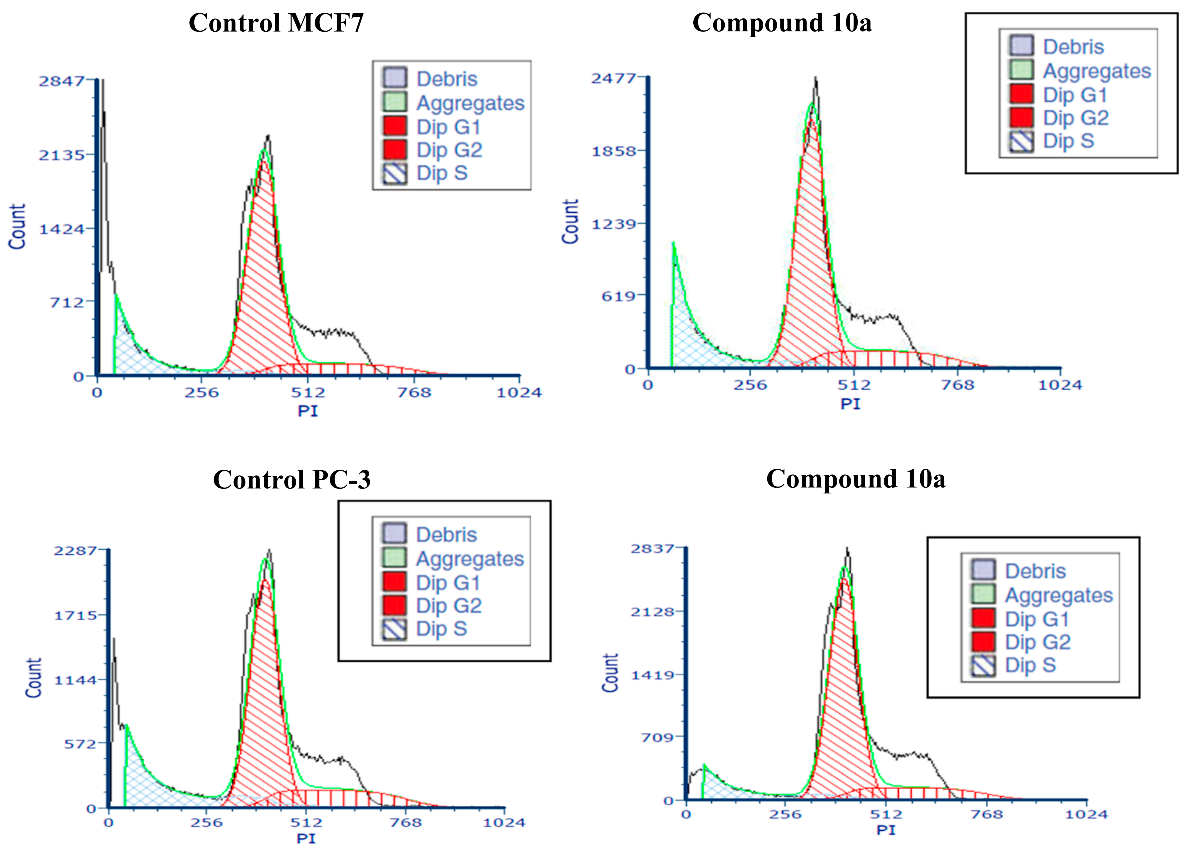

Fig. 4. Cell cycle assay and effect of compound 10a on MCF-7 (upper panel) and PC-3 cells (lower panel) evaluated by flow cytometry.

3.5. Structure activity correlation

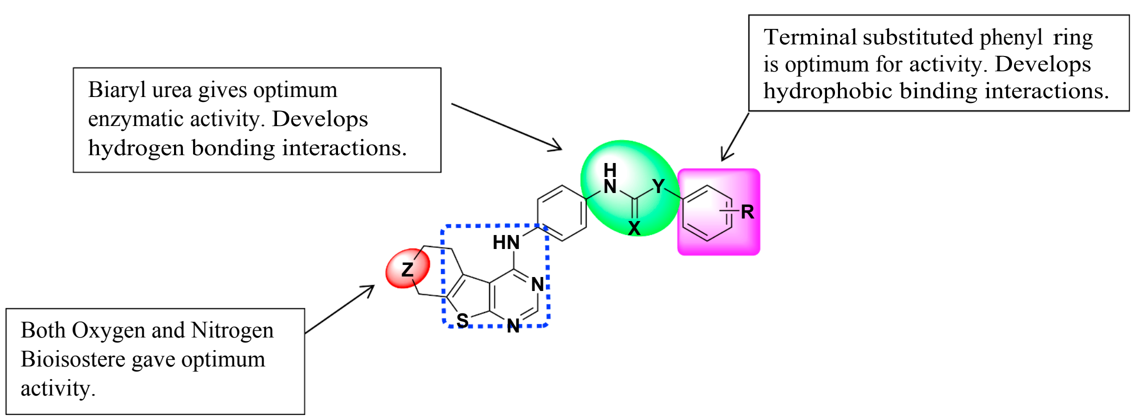

Structure activity relationship among the newly synthesized pyrano and pyrido thieno[2,3-*d*]pyrimidine derivatives has been closely investigated. As compared to the non-inhibitory activity exhibited by the amide derivative (**9c**) at 10 μM concentration it was revealed that the incorporation of the biarylurea moiety in the rest of the compounds (**10a-f,l,m,14a,d,e,15a-m**) resulted in significant increase in enzymatic activity in the different thienopyrimidine series.

The removal of the bulky protective group from compounds (**14a,d,e**) showed noticeable increase in the inhibitory activity in all of the tested compounds (**15a-m**). Moreover the systematic investigation of various substituents incorporated especially at 3- or 4- position of the terminal phenyl ring was generally well tolerated and resulted in considerable increase in the inhibitory activity. Noticeably, di substitutions in the 3- and 4-positions of the terminal phenyl ring like 3-CF_3, 4-Cl (**10d,15d**) and 3-Cl, 4-CH_3 derivatives (**10e,15e**) exhibited the highest inhibition percent ranging from 61 to 85% at 10 μM concentration. The absence of substituents in terminal phenyl ring abolished the kinase inhibitory activity as in derivatives (**10a,f,14a,15a).**

Further investigations of the biological results concluded that the thiourea derivative (**10f**) incorporating the pyran ring didn't show superiority in activity over the urea derivatives (**10a-e,l,m**) while in the pyridothienopyrimidine series compounds incorporating thiourea showed noticeable high inhibitory activity ranging from 78 to 85%. (**15f, g**). Finally it can be concluded that the substitution on the nitrogen of the pyridine ring decreased the enzymatic activity and removal of the tertiary butyl moiety significantly increased the biological activity. (**14d&15d**)

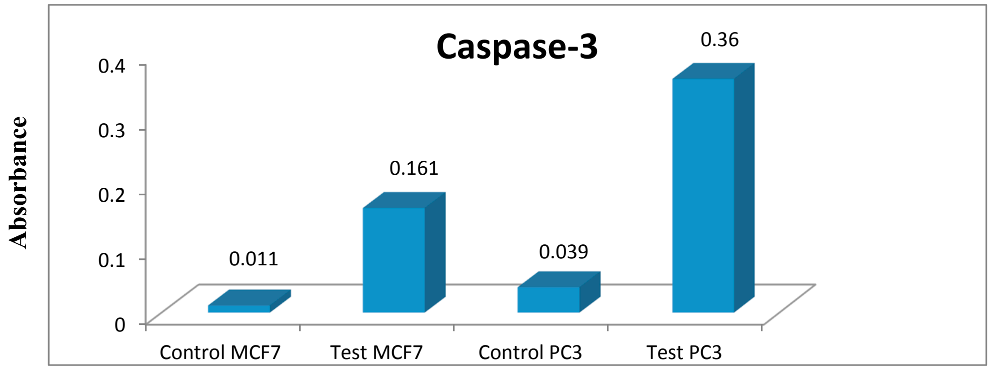

Fig. 5. Caspase-3 absorbance data obtained for compound 10a on both MCF-7 and PC-3 cell lines compared with control.

Generally the monosubstituted derivatives (**10b,10c,10l,10m,15i, 15j, 15k, 15l**) showed weak to moderate inhibition. Derivatives bearing 3-CH_3, 3-OCH_3, 3F and 4F (**10b,c,l,m**) showed 7, 12, 8, 13% inhibition respectively. On the other hand, the 4-Br, 4-OCH_3, 4-Cl, 4-F, of the pyridothienopyrimidine series exhibited moderate to good inhibitory activity ranging from 30 to 70% at the same concentration.

4. Molecular modeling studies

4.1. Docking study

Molecular modeling simulation study was performed through docking of the target compounds in the binding site of VEGFR-2 enzyme using C-Docker protocol in Discovery Studio 4.1 Software. In this investigation, docking study on the target compounds and analysis of their binding modes was performed to interpret the biological results and to gain further insight into binding orientations and interactions. The selected docking pose among the 10 retrieved possible ones was chosen based on the similarity of its binding mode to that of the co-crystallized ligand.

It is worth noting that the X-ray crystallographic enzyme (VEGFR-2) substrate (pyrrolo[3,2-*d*]pyrimidine lead compound (**III**)) complex of PDB code **(3VHE)**, revealed a hydrogen bond formed with Cys919 in the hinge region. The urea moiety interacted with the protein through two hydrogen bonds; the two NH formed bifurcate hydrogen bonds with Glu885 residue while the urea carbonyl forms hydrogen bond with Asp1046 residue. The substituted phenyl ring lied in a deep extended hydrophobic pocket created by the movement of Phe1047 residue of the 'DFG' motif to induce the 'DFG-out' conformation.

Validation of C-Docker protocol used in this study was performed by re-docking the lead compound **(III)** in the VEGFR-2 kinase active site. This was followed by the alignment of the X-ray bioactive [15] conformer of the lead compound with the best fitted pose achieved from the docking run. The alignment showed good coincidence between them with RMSD = 0.5 Å, indicating the ability of the used docking protocol to retrieve valid docking poses Fig. 6.

The docking study of the synthesized compounds into VEGFR-2 active site revealed comparable binding modes of the docked molecules

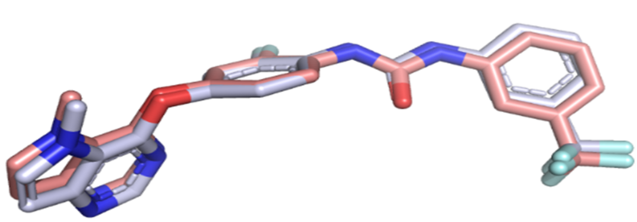

Fig. 6. The alignment between the X-ray bioactive conformer of the lead compound (III) (colored in pink) and the docked pose of the same compound (colored in blue) at VEGFR-2 binding site.

to the lead compound. Moreover, most of them showed higher docking scores relative to that of the docked lead compound.

Docking of the target compounds showed that the core scaffolds adopted volumes and orientation as the lead compound. Compounds with urea linkage **(10a-f, 10l,m 14a-m, 15a-m)** fulfilled the key interactions, where the hydrogen bonds with Cys919, Glu 885, Asp1046 residues were established.

These findings further interpreted the potent VEGFR-2 inhibitory activity observed for the urea-based derivatives when compared with the amide derivatives. This was also consistent with the previously reported SAR studies on various VEGFR-2 inhibitors, which revealed that the substituted biarylurea moiety is favorable for optimal interaction with the hydrophobic back pocket of VEGFR-2 kinase. On the other hand, derivatives bearing the amide tail **(9a-d)**, missed the key interaction with Glu885 residue which is regarded as an essential feature for type-II inhibitors. This interprets their weaker VEGFR-2 kinase inhibitory activity in the kinase assay. The binding interactions of the docked compounds together with their binding energies are presented below in Fig. 7 (Fig. 7**e–n** of SM).

4.2. In silico ADMET predictive study

In order to further investigate pharmacokinetics properties of synthesized compounds, computer-aided ADMET study was performed by using Accelrys Discovery Studio 2.5 software protocols through which we could predict absorption, distribution, metabolism, excretion and toxicity properties of the proposed molecules. This study was based on the chemical structure of the molecule and involves the calculation of certain pharmacokinetic parameters.

The results of the ADME study are presented as ADME-Plot, which is a 2D plot drawn using calculated PSA_2D and A logp98 properties. Blood Brain Barrier (BBB) Fig. 8.

The ADME study was used to compare the pharmacokinetic properties of the newly synthesized thieno[2,3*d*] pyrimidine derivatives bearing oxygen and nitrogen congeners **(10b,10c,10e)** with the lead compounds (**I** and **III**) the findings showed that the new synthesized compounds as the cyclic ethers have improved pharmacokinetic properties together with better aqueous solubility and better absorption levels. The calculated parameters from the ADMET study are tabulated in (Table 1 of SM).

5. Conclusion

Series of pyrimidine-based derivatives namely pyrido and pyranothieno[2,3-*d*]pyrimidine series, linked to either biarylamide or biarylurea or thiourea were designed, synthesized and evaluated for their *in vitro* VEGFR-2 inhibitory activity as well as their anti-proliferative activity against NCI 60 cell line panel. Most of the biarylurea and thiourea-based derivatives linked to the fused pyrimidine scaffolds exhibited moderate to good VEGFR-2 inhibition at 10 μM

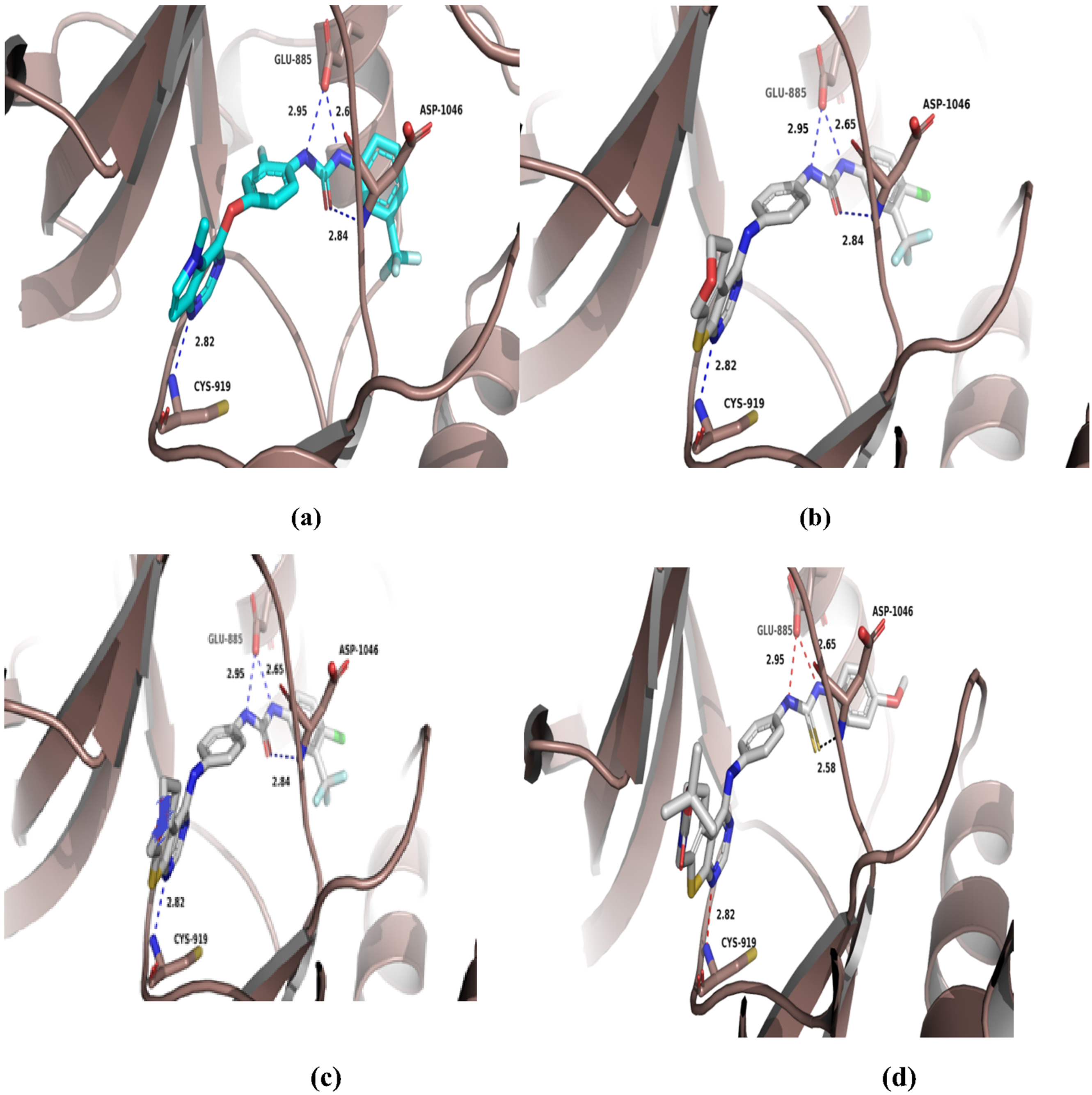

Fig. 7. **(a)** Retrieved docking pose of the pyrimidine-based inhibitor **(III)** (PDB code 3VHE) showing the same key interactions as reported. **(b–d)** Docking poses of the target compounds (**10d, 15d, 15 g**) to the ATP binding pocket of VEGFR-2 in its inactive conformation, all of the compounds established the same key interactions as the lead compound.

concentration, while derivatives bearing di substitutions on the terminal phenyl ring generally exhibited better VEGFR-2 inhibition compared to their mono substituted analogues. The pyranothieno[2,3-*d*] pyrimidine derivative **10d** manifested good *in vitro* kinase inhibitory activity (IC_{50} 2.5 μM), while compound **10e** exhibited 73% inhibition on VEGFR-2.

Furthermore in the pyridothieno[2,3-*d*]pyrimidine series both compounds **15d** and **15 g** showed high inhibitory activity on VEGFR-2 of (IC_{50} 5.48 μM, 2.27 μM), respectively. Moreover some of the synthesized compounds **15b,c,e,f,h,i,k,l,m** showed moderate inhibitory activity ranging from 50 to 80% inhibition on VEGFR-2. Compound **10a** exhibited significant cell growth inhibition on some specific NCI cell lines, especially those of breast, prostate, renal, ovarian, CNS, colon and non-small lung cancers. On the other hand, the amide-based derivatives **(9a-d)** showed no inhibition on VEGFR-2 (0%) at 10 μM concentration.

Molecular docking studies also explained these results; they revealed the ability of the urea-based derivatives to form a network of key interactions, known to be essential for type II VEGFR-2 inhibitors. However, their amide-based analogues missed one key interaction with Glu 885 residue.

6. Experimental

Starting materials, reagents and solvents were purchased from Sigma-Aldrich (USA) or Alfa-Aesar Organics and used without further purification. Reactions were monitored by analytical thin layer

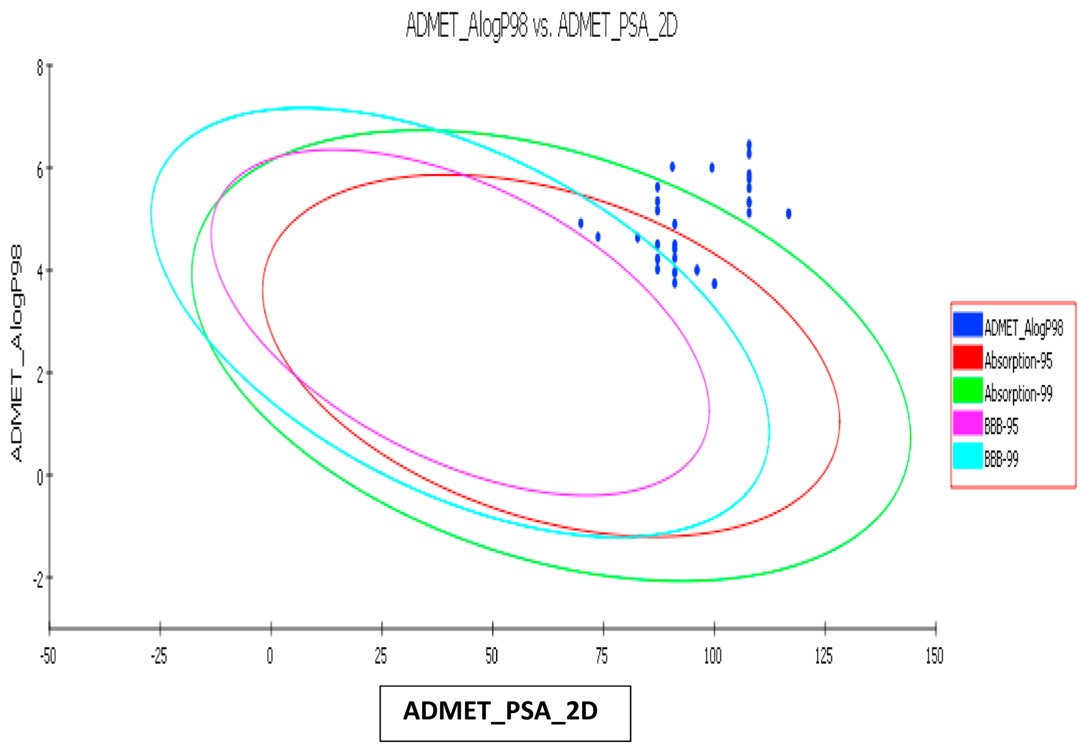

Fig. 8. ADME plot for the newly designed compounds.

chromatography (TLC), performed on silica GF254 plates packed on Aluminium sheets, purchased from (E. Merck, Germany) with visualization under U.V. light (254 nm). Melting points (°C) were determined by open capillary tube method using (Bio Cote SMP 10) apparatus and they are uncorrected. Mass spectrum was carried out on Direct Inlet part to mass analyzer in Thermo Scientific GCMS model ISQ at the Regional Center for Mycology and Biotechnology (RCMB), Al-Azhar University, Nasr City, Cairo. ^{1}H and ^{13}C NMR spectra were recorded in δ scale given in ppm on a Bruker Avance III HD FT-high resolution-NMR 400 MHz at the Center for Drug Discovery Research and Development, Faculty of Pharmacy, Ain Shams University. Chemical shifts (δH) are reported relative to TMS as internal standard. All coupling constant (J) values are given in Hertz. Chemical shifts (δC) are reported relative to DMSO-d_6 as internal standards. The abbreviations used are as follows: s: singlet; d: doublet; t: triplet; q: quartet and m: multiplet. IR spectra were recorded on Schimadzu FT-IR 8400S spectrophotometer at Faculty of Pharmacy-Ain Shams University. Elemental analyses were performed at the Regional Center for Mycology and Biotechnology, Al-Azhar University.

Thin layer chromatography was performed on precoated (0.25 mm) silica gel GF254 plates (E. Merck, Germany), compounds were detected with 254 nm UV lamp. Silica gel (60–230 mesh) was employed for routine column chromatography separations. *In vitro* antitumor testing was conducted at the NCI's disease-oriented human cell lines assay facility, Bethesda, MD, USA. Cell Cycle analysis of the effect of compound **10a** on both MCF-7 breast cancer and PC-3 prostate cancer cell lines was performed at VACSERA, Egypt.

Molecular modeling study was conducted using Discovery Studio Client version 4.1 software. Enzyme structure, starting coordinates of VEGFR-2 enzyme complexes with pyrolo pyrimidine (PDB code **3VHE**).

6.1. Chemistry

Data of the reported intermediates are presented in Supplementary Materials.

6.1.1. General procedure for preparation of substituted N-(4-nitrophenyl) benzamides *1a-e*

The key intermediates were synthesized according to the pathways described in Schemes 1a and 1b. To a stirred solution of *p*-nitroaniline (1 g, 7.24 mmol:1 equiv.) in pyridine (5 mL), the appropriate acid chloride (1.5 mL, 9.41 mmol:1.3 equiv.) was added dropwise and the mixture was stirred at room temperature for 24 h. The progress of the reaction was monitored by TLC. Water (100 mL) was then added to the mixture, and the resulting precipitate was collected by filtration. Crystallization of the precipitate from ethanol/methanol gave yellow needles (70–85%) of **1a-e** [28].

6.1.2. General procedure for preparation of substituted (4-Aminophenyl) benzamides *2a-e*

To a solution of the appropriate nitro derivatives **1a-e** (1 g, 3.6 mmol) in absolute ethanol or methanol (100 mL), Pd-C (0.1 g, 10%) was added then the mixture was stirred under H_2 at room temperature, for 30 min. After removing the catalyst by filtration over Celite, the filtrate was concentrated in vacuo, and dried to afford the crystals of compounds **2a-e** which were crystallized from methanol (65–85%).

6.1.3. General procedure for preparation of 1-(4-Nitrophenyl)-3-substituted phenylureas and thioureas *3a-m* [36]

To a solution of *p*-nitroaniline (1 g, 7.24 mmol; 1equiv.) in dry DCM (20 mL), the appropriate isocyanate (6 mmol; 1 equiv.) was added and the mixture was stirred at room temperature for 24 h. The reaction mixture was concentrated in vacuo, to afford the yellowish white crystals of compounds **3a-g**. Recrystallization from ethanol gave compounds **3a-g** in affordable yields (55–85%). **Method A.** Meanwhile compounds **3h-m** were prepared by **Method B** in which 4-Nitrophenyl isocyanate (6 mmol) was stirred in THF (10 mL) then the appropriate substituted anilines (7.2 mmol, 2equiv) were added dropwise. The mixture was heated and stirred at 60 °C for 24 h followed by the addition of few drops of triethylamine to the reaction mixture to give the targeted nitrophenyl urea derivatives **3h-m**. The solid was separated by filtration, dried and crystallized from dichloromethane without further purification [23].

*6.1.3.1. 1-(3,4-Dichlorophenyl)-3-(4-nitrophenyl)urea **3h***. The entitled compound was separated as yellow to white crystals. (1 g, 50%) m.p. > 300 °C **^{1}H NMR (400 MHz, $CDCl_3$)** δ 9.53 (s, 1H, NH D_2O exchangeable), 9.26 (s, 1H, NH D_2O exchangeable), 8.20 (d, J = 8 Hz, 2H, ArH), 8.17 (d, J = 8 Hz, 2H, ArH), 7.69 (s, 1H, ArH), 7.62 (d, J = 8 Hz, 1H, ArH), 7.56 (d, J = 8 Hz, 1H, ArH).

*6.1.4. General procedure for preparation of 1-(4-Aminophenyl)-3-substituted phenylurea **4a-m***

General procedure:

To a solution of the appropriate nitrophenyl urea derivatives **(3a-m)** (4 mmol) in the appropriate solvent either methanol or ethanol (100 mL), Pd-C (0.1 g, 10%) was added and the mixture was stirred under H_2 at room temperature, for 30–60 min. After removing the catalyst by filtration over Celite, the filtrate was concentrated *in vacuo*, dried to afford the crystals of compounds **(4a-m)** in yields (55–78%) which were recrystallized from ethanol.

*6.1.4.1. 1-(4-Aminophenyl)-3-(3,4-dichlorophenyl)urea **(4h)***. White crystals. (0.57 g, 64%); m.p. > 300 °C **^{1}H NMR (400 MHz, $CDCl_3$)** δ 8.80 (s, 1H, NH D_2O exchangeable), 8.26 (s, 1H, NH D_2O exchangeable), 7.87 (s, 1H, ArH), 7.49 (d, J = 8 Hz, 1H, ArH), 7.30 (d, J = 8 Hz, 1H, ArH), 7.08 (d, J = 8 Hz, 2H, ArH), 6.53 (d, J = 8 Hz, 2H, ArH), 4.82 (s, 2H, NH D_2O exchangeable). **MS**: (Mwt.: 295): *m/z*, 297 [M^+ +2, (18%)], 294.76 [M^+, (54%)].

*6.1.5. 2-Amino-5,7-dihydro-4H-thieno[2,3-c]pyran-3-carbonitrile **(7)** [44]*

A mixture of tetrahydro-4*H*-pyran-4-one (1 g, 10 mmol:1 equiv.) malononitrile (0.65 g, 10 mmol:1 equiv.), and sulfur powder (0.32 g, 10 mmol:1 equiv.) were mixed in absolute ethanol (10 mL). Morpholine (1 equiv) was added dropwise over a period of 30 min to the reaction mixture which was heated and stirred in water bath at 50–60 °C overnight. The mixture was then added to ice/water with continued stirring. The resulting crystalline product washed with water and recrystallized from ethanol to give the titled product **(7)** as brown crystals (1.2 g, 66%); m.p. 225–227 °C (as reported) [44]. **^{1}H NMR (400 MHz, DMSO-d_6)** δ 7.10 (s, 2H, NH D_2O exchangeable), 4.42 (s, 2H, <u>CH$_2$</u> pyran), 3.83 (t, 2H, J = 4 Hz, <u>CH$_2$</u> pyran), 2.44 (t, 2H, J = 4 Hz, <u>CH$_2$</u> pyran).

*6.1.6. N′-(3-Cyano-5,7-dihydro-4H-thieno[2,3-c]pyran-2-yl)-N,N-dimethylformamidine **(8)***

A solution of 2-amino-5,7-dihydro-4*H*-thieno[2,3-*c*]pyran-3-carbonitrile **(8)** (1gm 5.5 mmol:1equiv.) in *N,N*-dimethylformamide dimethylacetal (2.63 gm, 2.93 mL, 22.1 mmol:4 equiv.) was heated under reflux for 5–9 h. The disappearance of the starting material was judged by TLC, the reaction mixture was allowed to cool at room temperature. The formed solid was washed with diethyl ether (2 * 15 mL) allowed to air dry and crystallized from ethanol to yield **8** as brown gold crystals. (0.9 g, 69%) **^{1}H NMR (400 MHz, $CDCl_3$)** δ 7.71 (s, 1H −<u>CH</u>═N−), 4.61 (s, 2H, <u>CH$_2$</u> pyran), 3.99 (t, 2H, J = 4 Hz, <u>CH$_2$</u> pyran), 3.14 (s, 6H, N (<u>CH$_3$</u>)$_2$, 2.70 (t, 2H, J = 4 Hz, −<u>CH$_2$</u> pyran). **FT-IR (ύ max, cm^{-1})**: 2958 (CH aliphatic), 2203 (C≡N), 1633 (C═N).

*6.1.7. General procedure for preparation of N-(4-((5,8-Dihydro-6H-pyrano [4′,3′:4,5] thieno [2,3-d]pyrimidin-4-yl)amino)phenyl) substituted benzamide **9a-d***

A mixture of **8** (0.5 gm, 2.12 mmol) and the respective (4-aminophenyl) substituted benzamide **2a-d** (2.5 mmol:1.2equiv) was stirred and heated under reflux for 5–8 h, in acetic acid (2 mL). The reactions were monitored by TLC. After the reaction was completed the formed solid was either filtered or condensed under *vacuo* and finally washed with diethyl ether and allow to air dry. **9a-d** (30–40%).

*6.1.7.1. N-(4-((5,8-Dihydro-6H-pyrano[4′,3′:4,5]thieno[2,3-d]pyrimidin-4-yl)amino)phenyl) benzamide **(9a)***. Brown crystals (0.3 g, 35%); m.p. 240–242 °C; **^{1}H NMR (400 MHz, DMSO-d_6)** δ 8.66 (s, 1H, NH D_2O exchangeable), 8.60 (s, 1H, NH D_2O exchangeable), 8.37 (s, 1H, pyrimidine H), 7.54 (d, J = 8 Hz, 2H, ArH), 7.47 (t, J = 8 Hz, 2H, ArH), 7.37 (d, J = 8 Hz, 2H, ArH), 7.28 (d, J = 8 Hz, 2H, ArH), 6.98 (t, J = 8 Hz, 1H, ArH), 4.84 (s, 2H, −<u>CH$_2$</u> pyran), 4.0 (t, 2H, J = 4 Hz, −<u>CH$_2$</u> pyran), 3.25 (t, J = 4 Hz, 2H, <u>CH$_2$</u> pyran); **Anal**. Calcd for $C_{22}H_{18}N_4O_2S$ (Mwt.: 402.12): C, 65.65; H, 4.51; N, 13.92; O, 7.95; S, 7.97 Found C, 65.47; H, 4.38; N, 13.78; O, 7.79; S, 7.85.

*6.1.7.2. 4-Chloro-N-(4-((5,8-dihydro-6H-pyrano[4′,3′:4,5]thieno[2,3-d] pyrimidin-4-yl)amino)phenyl)benzamide **(9b)***. Buff crystals (0.32 g, 32%); m.p. > 300 °C; **^{1}H NMR (400 MHz, DMSO-d_6)** δ 10.45 (s, 1H, NH D_2O exchangeable), 10.27 (s, 1H, NH D_2O exchangeable), 8.63 (s, 1H, pyrimidine H), 7.99 (d, J = 8 Hz, 2H, ArH), 7.88 (d, J = 8 Hz, 2H, ArH), 7.56 (d, J = 8 Hz, 2H, ArH), 7.35 (d, J = 8 Hz, 2H, ArH), 4.90 (s, 2H, −<u>CH$_2$</u> pyran), 3.99 (t, 2H, J = 4 Hz, −<u>CH$_2$</u> pyran), 2.04 (t, J = 4 Hz, 2H, <u>CH$_2$</u> pyran). **Anal**. Calcd for $C_{22}H_{17}ClN_4O_2S$ (Mwt.: 436.91): C, 60.48; H, 3.92; Cl, 8.11; N, 12.82; O, 7.32; S, 7.34. Found C, 60.66; H, 3.79; Cl, 8.26; N, 12.72; O, 7.56; S, 7.48.

*6.1.7.3. 4-Bromo-N-(4-((5,8-dihydro-6H-pyrano[4′,3′:4,5]thieno[2,3-d] pyrimidin-4-yl)amino)phenyl)benzamide **(9c)***. Orange crystals (0.38 g, 30%); m.p. > 300 °C; **^{1}H NMR (400 MHz, DMSO-d_6)** δ 10.23 (s, 1H, NH D_2O exchangeable), 10.03 (s, 1H, NH D_2O exchangeable), 8.81 (s, 1H, pyrimidine H), 7.97 (d, J = 8 Hz, 2H, ArH), 7.70 (d, J = 8 Hz, 2H, ArH), 7.58 (d, J = 8 Hz, 2H, ArH), 7.54 (d, J = 8 Hz, 2H, ArH) 4.62 (s, 2H, −<u>CH$_2$</u> pyran), 3.15 (t, 2H, J = 4 Hz, −<u>CH$_2$</u> pyran), 2.04 (t, J = 4 Hz, 2H, <u>CH$_2$</u> pyran). **Anal**. Calcd for $C_{22}H_{17}BrN_4O_2S$ (Mwt.: 480.03): C, 54.66; H, 3.43; Br, 16.72; N, 11.55; O, 6.58; S, 6.84 Found C, 54.76; H, 3.48; Br, 16.47; N, 11.52; O, 6.59; S, 6.89.

*6.1.7.4. N-(4-((5,8-Dihydro-6H-pyrano[4′,3′:4,5]thieno[2,3-d]pyrimidin-4-yl)amino)phenyl)-4-methoxybenzamide **(9d)***. Orange crystals (0.39 g, 32%); m.p. 248–249 °C; **^{1}H NMR (400 MHz, DMSO-d_6)** δ 9.85 (s, 2H, NH D_2O exchangeable), 8.37 (s, 1H, pyrimidine H), 7.96 (d, J = 8 Hz, 2H, ArH), 7.67 (d, J = 8 Hz, 2H, ArH), 7.54 (d, J = 8 Hz, 2H, ArH), 7.05 (d, J = 8 Hz, 2H, ArH) 4.84 (s, 2H, −<u>CH$_2$</u> pyran), 3.99 (t, 2H, J = 4 Hz, −<u>CH$_2$</u> pyran), 3.73 (s, 3H, Ph-<u>OCH$_3$</u>), 3.12 (t, J = 4 Hz, 2H, <u>CH$_2$</u> pyran). **Anal**. Calcd for $C_{23}H_{20}N_4O_3S$ (Mwt.: 432.50): C, 63.87; H, 4.66; N, 12.95; O, 11.10; S, 7.41 Found C, 63.75; H, 4.52; N, 12.73; O, 11.22; S, 7.67.

*6.1.8. General procedure for preparation of 1-(4-((5,8-Dihydro-6H-pyrano [4′,3′:4,5] thieno[2,3-d]pyrimidin-4-yl)amino)phenyl)-3-(substituted phenyl) urea and thiourea. **10 a-f,l,m***

General procedure:

A mixture of 8 (0.3 gm, 2.12 mmol) and the respective 1-(4-aminophenyl)-3- substituted phenylureas **4a-e,l,m** or thiourea **4f** (2.5 mmol:1.2equiv.) was stirred and heated under reflux for 4–8 h in acetic acid (2 mL). Reaction completion was judged by TLC. The reaction mixture was filtered while hot. The resultant solid was washed with diethyl ether and allow to air dry. The final products were purified either by crystallization from an appropriate solvent or by column chromatography using Hex-EtOAc (7:3) as an eluent. **10 a-f,l,m**.

*6.1.8.1. 1-(4-((5,8-Dihydro-6H-pyrano[4′,3′:4,5]thieno[2,3-d]pyrimidin-4-yl)amino)phenyl)-3-phenylurea **(10a)***. Brown crystals (0.35 g, 39%); m.p. 235–236 °C; **^{1}H NMR (400 MHz, DMSO-d_6)** δ 8.66 (s, 1H, NH D_2O exchangeable), 8.60 (s, 1H, NH D_2O exchangeable), 8.52 (s, 1H, NH D_2O exchangeable), 8.37 (s, 1H, pyrimidine H), 7.54 (d, J = 8 Hz, 2H, ArH), 7.47 (t, J = 8 Hz, 2H, ArH), 7.37 (d, J = 8 Hz, 2H, ArH), 7.28 (d, J = 8 Hz, 2H, ArH), 6.98 (t, J = 8 Hz, 1H, ArH), 4.84 (s, 2H, −<u>CH$_2$</u> pyran), 4.0 (t, 2H, J = 4 Hz, −<u>CH$_2$</u> pyran), 3.25 (t, J = 4 Hz, 2H, <u>CH$_2$</u> pyran); **^{13}C NMR (100 MHz, DMSO-d_6)** δ 166.47, 155.70, 153.04, 152.97, 136.24, 134.52, 130.72, 129.21, 129.20, 125.08, 123.92, 123.49, 122.07, 120.08, 119.55, 119.42, 118.78, 118.58, 118.52, 65.17, 64.36, 26.43. **Anal**. Calcd for $C_{22}H_{19}N_5O_2S$ (Mwt.: 417.49): C, 62.13; H, 4.78; N, 15.09; S, 6.91; C, 63.29; H, 4.59; N, 16.78; O, 7.66; S, 7.68; Found C, 62.10; H, 4.75; N, 15.11; S, 6.89; C, 63.26; H, 4.55; N, 16.786; O, 7.65; S, 7.65 **FT-IR (ύ max, cm^{-1})**: 3300 (NH), 3075 (CH aromatic), 2922 (CH aliphatic), 1685 (C=O amide), 1633 (C=N).

*6.1.8.2. 1-(4-((5,8-Dihydro-6H-pyrano[4′,3′:4,5]thieno[2,3-d]pyrimidin-4-yl)amino)phenyl)-3-(m-tolyl)urea **(10b)***. The titled compound was purified by column chromatography to obtain buff crystals. (0.35 g, 38%); m.p. > 300 °C. **^{1}H NMR (400 MHz, DMSO-d$_6$)** δ 9.93 (s, 1H, NH D_2O exchangeable), 9.82 (s, 1H, NH D_2O exchangeable), 8.52 (s, 1H, NH D_2O exchangeable), 8.37 (s, 1H, pyrimidine H), 8.14 (d, J = 8 Hz, 1H, ArH), 7.55 (s, 1H, ArH) 7.47 (d, J = 8 Hz, 2H, ArH), 7.37 (d, J = 8 Hz, 2H, ArH), 7.15 (t, J = 8 Hz, 1H, ArH) 6.79 (d, J = 8 Hz, 1H, ArH), 4.84 (s, 2H, $\underline{CH_2}$ pyran), 3.99 (t, J = 4 Hz, 2H, $\underline{CH_2}$, pyran), 3.24 (t, J = 4 Hz, 2H, $\underline{CH_2}$ pyran), 2.28 (s, 3H, Ph-$\underline{CH_3}$). **^{13}C NMR (100 MHz, DMSO-d$_6$)** δ 168.70, 156.82, 154.76, 148.01, 139.59, 137.26, 135.56, 134.28, 130.07, 128.94, 125.62, 122.75, 122.35, 120.22, 119.98, 119.82, 119.61, 119.59, 119.42, 65.19, 64.37, 26.62, 21.96. **Anal**. Calcd for $C_{23}H_{21}N_5O_2S$ (Mwt.: 431.51): C, 64.02; H, 4.91; N, 16.23; O, 7.42; S, 7.43; Found C, 64.07; H, 4.94; N, 16.26; O, 7.40; S, 7.47; **FT-IR (ύ max, cm^{-1})**: 3299 (NH), 3038 (CH aromatic), 2915 (CH aliphatic), 1682 (C=O amide), 1633 (C=N).

*6.1.8.3. 1-(4-((5,8-Dihydro-6H-pyrano[4′,3′:4,5]thieno[2,3-d]pyrimidin-4-yl)amino)phenyl)-3-(3-methoxyphenyl)urea **(10c)***. Light brown crystals. (0.5 g, 52%); m.p. 208–210 °C. **^{1}H NMR (400 MHz, DMSO-d$_6$)** δ 9.81 (s, 1H, NH D_2O exchangeable), 8.61 (s, 1H, pyrimidine H), 8.51 (s, 2H, NH D_2O exchangeable), 7.48 (d, J = 8 Hz, 1H, ArH), 7.35 (d, J = 8 Hz, 2H, ArH), 7.19 (t, J = 8 Hz, 1H, ArH), 7.15 (s, 1H, ArH), 6.93 (d, J = 8 Hz, 1H, ArH), 6.55 (d, J = 8 Hz, 2H, ArH), 4.84 (s, 2H, $\underline{CH_2}$ pyran), 3.99 (t, J = 4 Hz, 2H, $\underline{CH_2}$ pyran), 3.74 (s, 3H,Ph-$\underline{OCH_3}$), 3.24 (t, 2H, J = 4 Hz, $\underline{CH_2}$ pyran). **^{13}C NMR (100 MHz, DMSO-d$_6$)** δ 168.98, 160.04, 155.66, 153.34, 141.96, 140.33, 132.26, 130.47, 130.33, 125.18, 119.45, 118.99, 115.09, 110.89, 109.59, 107.94, 107.57, 107.23, 102.51, 65.19, 64.37, 55.38, 26.62. **Anal**. Calcd for $C_{23}H_{21}N_5O_3S$ (Mwt.: 447.14): C, 61.73; H, 4.73; N, 15.65; O, 10.73; S, 7.16; Found C, 61.70; H, 4.70; N, 15.61; O, 10.70; S, 7. **FT-IR (ύ max, cm^{-1})**: 3299 (NH), 3056 (CH aromatic), 2988 (CH aliphatic), 1678 (C=O amide), 1620(C=N).

*6.1.8.4. 1-(4-Chloro-3-(trifluoromethyl)phenyl)-3-(4-[(5,8 dihydro-6H-pyrano[4′,3′:4,5] thieno[2,3-d]pyrimidin-4-yl)amino]phenyl)urea **(10d)***. The reaction mixture was evaporated under *vacuo*. The resulted solid was purified using column chromatography to give pale brown crystals. (0.44 g, 40%); m.p. > 300 °C; **^{1}H NMR (400 MHz, DMSO-d$_6$)** δ 9.93 (s, 1H, NH D_2O exchangeable), 9.85 (s, 2H, NH D_2O exchangeable), 8.37 (s, 1H, pyrimidine H), 8.17 (d, J = 8 Hz, 1H, ArH), 7.56 (s, 1H, ArH), 7.47 (m, 4H, ArH), 7.38 (d, J = 8 Hz, 1H, ArH), 4.87 (s, 2H, $\underline{CH_2}$ pyran), 3.98 (t, J = 4 Hz, 2H, $\underline{CH_2}$ pyran), 3.23 (t, J = 4 Hz, 2H, $\underline{CH_2}$ pyran). **^{13}C NMR (100 MHz, DMSO-d$_6$)** δ 168.43, 168.31, 155.69, 155.56, 153.03, 135.85, 135.04, 134.59, 132.56, 132.24, 130.73, 100.93, 125.42, 125.08, 123.47, 120.06, 119.77, 119.54, 118.991, 112.814, 65.16, 64.35, 24.30. **Anal**. Calcd for $C_{23}H_{17}ClF_3N_5O_2S$ (Mwt.: 519.07): C, 53.13; H, 3.30; Cl, 6.82; F, 10.96; N, 13.47; O, 6.15; S, 6.17; Found C, 53.12; H, 3.33; Cl, 6.85; F, 10.91; N, 13.42; O, 6.10; S, 6.12 **FT-IR (ύ max, cm^{-1})**: 3340 (NH), 3109 (CH aromatic), 2986 (CH aliphatic), 1685 (C=O amide), 1632 (C=N).

*6.1.8.5. 1-(3-Chloro-4-(methyl)phenyl)-3-(4-[(5,8 dihydro-6H-pyrano [4′,3′:4,5] thieno[2,3d] pyrimidin-4-yl)amino]phenyl)urea **(10e)***. Buff crystals (0.45 g, 46%) m.p. > 300 °C. **^{1}H NMR (400 MHz, DMSO-d$_6$)** δ 9.81 (s, 1H, NH D_2O exchangeable), 8.51 (s, 2H, NH D_2O exchangeable), 8.37 (s, 1H, pyrimidine H), 7.70 (s, 1H, ArH), 7.48 (d, J = 8, 1H, ArH), 7.32–7.36 (m, 4H, ArH), 7.09 (d, J = 8, 1H, ArH), 4.82 (s, 2H, $\underline{CH_2}$ pyran), 3.99 (t, J = 4 Hz, 2H, $\underline{CH_2}$ pyran), 3.38 (t, J = 4, 2H, $\underline{CH_2}$ pyran), 2.02 (s, 3H, Ph-$\underline{CH_3}$). **^{13}C NMR (100 MHz, DMSO-d$_6$)** δ 168.42, 141.83, 138.79, 138.39, 133.48, 131.49, 130.87, 129.57, 123.47, 120.17, 120.08, 119.77, 119.54, 119.31, 118.92, 118.61, 114.81, 54.59, 54.33, 26.58, 24.51. **MS**: (Mwt.: 465): *m/z*, 467 [M$^+$ + 2, (4%)], 465 [M$^+$, (12%)]; **Anal**. Calcd for $C_{23}H_{20}ClN_5O_2S$ (Mwt.: 465.1): C, 59.29; H, 4.33; Cl, 7.61; N, 15.03; O, 6.87; S, 6.88; Found C, 59.20; H, 4.30; Cl, 7.57; N, 15.06; O, 6.82; S, 6. **FT-IR (ύ max, cm^{-1})**: 3293 (NH), 3089 (CH aromatic), 2954 (CH aliphatic), 1685 (C=O amide), 1638 (C=N).

*6.1.8.6. 1-(4-((5,8-Dihydro-6H-pyrano[4′,3′:4,5]thieno[2,3-d]pyrimidin-4-yl)amino)phenyl)-3-phenylthiourea **(10f)***. Yellowish brown crystals (0.50 g, 54%); m.p. 268–270 °C; **^{1}H NMR (400 MHz, DMSO-d$_6$)** δ 10.57 (s, 1H, NH D_2O exchangeable), 8.39 (s, 1H, pyrimidine H), 8.20 (t, J = 8 Hz, 2H, ArH), 7.96 (d, J = 8 Hz, 2H, ArH), 7.84 (d, J = 8 Hz, 2H, ArH), 7.78 (t, J = 8 Hz, 1H, ArH), 6.72 (2H, NH, D_2O exchangeable), 6.61 (d, J = 8 Hz, 2H, ArH), 4.60 (s, 2H, −$\underline{CH_2}$ pyran), 3.88 (t, 2H, J = 4 Hz, −$\underline{CH_2}$ pyran), 2.60 (t, J = 4 Hz, 2H, $\underline{CH_2}$ pyran); **Anal**. Calcd for $C_{22}H_{19}N_5OS_2$ (Mwt.: 433.55): C, 60.95; H, 4.42; N, 16.15; O, 3.69; S, 14.79; Found 60.90; H, 4.40; N, 16.12; O, 3.65; S, 14.76.

*6.1.8.7. 1-(4-((5,8-Dihydro-6H-pyrano[4′,3′:4,5]thieno[2,3-d]pyrimidin-4-yl)amino)phenyl)-3-(3-fluorophenyl)urea **(10l)***. Brown crystals. (0.36 g, 32%); m.p > 300 **^{1}H NMR (400 MHz, DMSO-d$_6$)** δ 9.92 (s, 1H, NH D_2O exchangeable), 8.40 (s, 2H, NH D_2O exchangeable), 8.37 (s, 1H, pyrimidine H), 8.21 (d, J = 8 Hz, 1H, ArH), 8.13 (s, 1H, ArH), 7.63 (t, J = 8 Hz, 2H, ArH) 7.55 (*m*, 4H, ArH), 4.85 (s, 2H, $\underline{CH_2}$ pyran), 3.98 (t, J = 4 Hz, 2H, $\underline{CH_2}$ pyran), 2.95 (t, J = 4 Hz, 2H, $\underline{CH_2}$ pyran), **Anal**. Calcd for $C_{22}H_{18}FN_5O_2S$ (Mwt.: 435.12): C, 60.68; H, 4.17; F, 4.36; N, 16.08; O, 7.35; S, 7.36; Found C, 60.63; H, 4.14; F, 4.30; N, 16.10; O, 7.38 S, 7.32.

*6.1.8.8. 1-(4-((5,8-Dihydro-6H-pyrano[4′,3′:4,5]thieno[2,3-d]pyrimidin-4-yl)amino)phenyl)-3-(4-fluorophenyl)urea **(10m)***. Light brown crystals. (0.45 g, 48%); mp > 300 **^{1}H NMR (400 MHz, DMSO-d$_6$)** δ 9.97 (s, 1H, NH D_2O exchangeable), 9.92 (s, 1H, NH D_2O exchangeable), 9.83 (s, 1H, NH D_2O exchangeable), 8.35 (s, 1H, pyrimidine H), 7.58–7.56 (m, 4H, ArH), 7.09–7.06 (m, 4H, ArH), 4.81 (s, 2H, $\underline{CH_2}$ pyran), 3.95 (t, J = 4 Hz, 2H, $\underline{CH_2}$ pyran), 3.20 (t, J = 4 Hz, 2H, $\underline{CH_2}$ pyran). **^{13}C NMR (100 MHz, DMSO-d$_6$)** δ 173.12, 168.45, 166.51, 159.42, 155.58, 152.91, 136.17, 135.78, 135.04, 134.51, 130.81, 125.05, 123.47, 121.10, 119.78, 119.55, 116.34, 115.71, 115.49, 65.15, 64.34, 26.40. **Anal**. Calcd for $C_{22}H_{18}FN_5O_2S$ (Mwt.: 435.12): C, 60.68; H, 4.17; F, 4.36; N, 16.08; O, 7.35; S, 7.36; Found C, 60.62; H, 4.18; F, 4.32; N, 16.8; O, 7.34 S, 7.38.

*6.1.9. Tert-butyl 2-amino-3-cyano-4,5-dihydrothieno[2,3-c]pyridine-6(7H)-carboxylate **(12)** [45]*

A mixture of *N*-Boc piperidone (1 g, 5 mmol:1 equiv.) malononitrile (0.66 g, 0.55 mL,5 mmol:1 equiv.), sulfur powder (0.16 g, 5 mmol:1 equiv.) were mixed in absolute ethanol (10 mL). Morpholine (5 mL) was added dropwise over a period of 30 min to the reaction mixture in water bath at 50–60 °C overnight. The mixture was then added to ice/water with continued stirring. The resulting solid was filtered, washed with water and crystallized from ethanol to give the titled product **(12)** as pale yellow crystals (1 g, 71%) m.p. 193–195 °C (as reported) [45].

*6.1.10. Tert-butyl 3-cyano-2-((dimethylamino)methylidine amino)-4,5-dihydrothieno[2,3-c]pyridine-6(7H)-carboxylate **(13)***

A solution of *tert*-butyl 2-amino-3-cyano-4,5-dihydrothieno[2,3-*c*] pyridine-6(7H)-carboxylate **(12)** (1 gm 3.5 mmol:1 equiv.) in *N,N*-dimethylformamide dimethyl acetal (5 mL, 33.3 mmol) was stirred and heated under reflux for 5 h. The reaction mixture was allowed to cool at room temperature after its completion was judged by TLC. The formed crystals was washed with diethyl ether (2 * 15 mL) allowed to air dry and recrystallized from hexane to yield **(13)** as yellowish gold crystals. (0.8 g, 67%) **^{1}H NMR (400 MHz, CDCl$_3$)** δ 7.69 (s, 1H −CH=N−), 4.43 (s, 2H, pyridine), 3.69 (t, 2H, J = 4 Hz, pyridine), 3.11 (s, 6H, N(CH$_3$)$_2$, 2.61 (t, 2H, J = 4 Hz, pyridine), 1.50 (s, 9H, -Boc).

*6.1.11. General procedure for preparation of tert-butyl-4-((4-(3-substituted-phenyl)ureido)phenyl)amino)-5,8 dihydropyrido [4′,3′:4,5] thieno[2,3-d]pyrimidine-7(6H)-carboxylate **14a-m***

General procedure:

A mixture of **13** (0.3 gm, 0.89 mmol) and the respective 1-(4-aminophenyl)-3- substituted phenylurea or thiourea **(4a-m)** (1 mmol:1.2equiv.) was stirred and heated under reflux in acetic acid (5 mL) for 16–24 h. The reactions were monitored with TLC. After the reaction was completed the resulted solid was washed with diethyl ether, left to air dry. The compounds were purified either by crystallization from an appropriate solvent or by column chromatography using DCM-EtOAc (8:2) as an eluent in yields 30–63%.

*6.1.11.1. Tert-butyl-4-((4-(3-phenylureido)phenyl)amino)-5,8-dihydropyrido [4′,3′:4,5] thieno[2,3-d]pyrimidine-7(6H)-carboxylate **(14a)***. The titled compound was obtained by evaporating the reaction mixture to dryness; the residue was mixed with water (10 mL), and extracted with ethyl acetate (2 * 50 mL). The combined organic layer was separated, dried over anhydrous Na$_2$SO$_4$, filtered and the solvent was evaporated under vacuum to obtain buff crystals. (0.2 g, 43%); m.p. > 300 °C **^{1}H NMR (400 MHz, DMSO-d$_6$)** δ 9.0 (s, 2H, NH D$_2$O exchangeable), 8.93 (s, 1H, NH D$_2$O exchangeable), 8.36 (s, 1H, pyrimidine H), 7.48 (d, J = 8 Hz, 2H, ArH), 7.37 (m, 4H, ArH), 7.26 (t, J = 8 Hz, 2H, ArH), 6.94 (t, J = 8 Hz, 1H, ArH), 4.68 (s,2H, CH$_2$ pyridine), 3.70 (t, 2H, J = 4 Hz, CH$_2$ pyridine), 3.21 (t, 2H, J = 4 Hz, CH$_2$ pyridine), 1.46 (s, 9H, Boc). **Calcd** for C$_{27}$H$_{28}$N$_6$O$_3$S (Mwt.: 516.62): C, 62.77; H, 5.46; N, 16.27; O, 9.29; S, 6.21; Found C, 62.63; H, 5.50; N, 16.32; O, 9.32; S, 6.28.

*6.1.11.2. Tert-butyl-4-((4-(3-(m-tolyl)ureido)phenyl)amino)-5,8-dihydropyrido[4′,3′:4,5] thieno[2,3-d]pyrimidine-7(6H)-carboxylate **(14b)***. Brown crystals (0.2 g, 42%); mp > 300 °C. **^{1}H NMR (400 MHz, DMSO-d$_6$)** δ 9.92 (s, 2H, NH D$_2$O exchangeable), 9.84 (s, 1H, NH D$_2$O exchangeable), 8.37 (s, 1H, pyrimidine H), 8.34 (d, J = 8 Hz, 2H, ArH), 7.58 (s, 1H, ArH), 7.51 (d, J = 8 Hz, 2H, ArH), 7.23 (t, J = 8 Hz, 1H, ArH), 6.85 (d, J = 8 Hz, 1H, ArH), 6.58 (d, J = 8 Hz, 1H, ArH), 4.78 (t, J = 4 Hz,2H, CH$_2$ pyridine), 4.46 (s, 2H, CH$_2$ pyridine), 3.09 (t, 2H, J = 4 Hz, CH$_2$ pyridine), 2.11 (s, 3H, Ph-CH$_3$), 1.46 (s, 9H, Boc). **Calcd** for C$_{28}$H$_{30}$N$_6$O$_3$S (Mwt.: 530.65): C, 63.38; H, 5.70; N, 15.84; O, 9.04; S, 6.04; Found C, 63.52; H, 5.84; N, 15.76; O, 9.24; S, 6.18.

*6.1.11.3. Tert-butyl-4-((4-(3-(3-methoxyphenyl)ureido)phenyl)amino)-5,8-dihydropyrido [4′,3′:4,5] thieno[2,3-d]pyrimidine-7(6H)-carboxylate **(14c)***. Dark brown crystals. (0.3 g, 62%); mp > 300 °C. **^{1}H NMR (400 MHz, DMSO-d$_6$)** δ 9.94 (s, 2H, NH D$_2$O exchangeable), 9.62 (s, 1H, NH D$_2$O exchangeable), 8.35 (s, 1H, pyrimidine H), 7.48–7.56 (m, 4H, ArH), 7.28 (s, 1H, ArH), 7.16 (d, J = 8 Hz, 1H, ArH), 7.02 (t, J = 8 Hz, 1H, ArH) 6.59 (d, J = 8 Hz, 1H, ArH), 4.77 (s, 2H, CH$_2$ pyridine), 3.69 (t, 2H, J = 4 Hz, CH$_2$ pyridine), 3.10 (t, 2H, J = 4 Hz, CH$_2$ pyridine), 3.72 (s, 3H, Ph-OCH$_3$), 2.03 (s, 9H, -Boc). **Calcd** for C$_{28}$H$_{30}$N$_6$O$_4$S (Mwt.: 546.65) C, 61.52; H, 5.53; N, 15.37; O, 11.71; S, 5.86; Found C, 61.38; H, 5.39; N, 15.29; O, 11.58; S, 5.69.

*6.1.11.4. Tert-butyl 4-((4-(3-(4-chloro-3-(trifluoromethyl)phenyl)ureido)phenyl)amino)-5,8-dihydropyrido[4′,3′:4,5]thieno[2,3-d]pyrimidine-7(6H)-carboxylate **(14d)***. Buff crystals. (0.3 g, 54%); mp > 300 °C. **^{1}H NMR (400 MHz, DMSO-d$_6$)** δ 9.72 (s, 1H, NH D$_2$O exchangeable), 9.03 (s, 1H, NH D$_2$O exchangeable), 8.97 (s, 1H, NH D$_2$O exchangeable), 8.43 (s, 1H, pyrimidine H), 7.47 (d, J = 8 Hz,1H, ArH), 7.38 (d, J = 8 Hz, 1H, ArH), 7.30 (s, 1H, ArH), 7.07 (d, J = 8 Hz, 2H, ArH) 6.86 (d, J = 8 Hz, 1H, ArH), 6.88 (d, J = 4 Hz, 1H, ArH), 3.86 (s, 2H, CH$_2$ pyridine), 2.66 (t, 2H, J = 4 Hz, CH$_2$ pyridine), 2.31 (t, 2H, J = 4 Hz, CH$_2$ pyridine), 1.42 (s, 9H, -Boc). **Calcd** for C$_{28}$H$_{26}$ClF$_3$N$_6$O$_3$S (Mwt.: 619.06) C, 54.33; H, 4.23; Cl, 5.73; F, 9.21; N, 13.58; O, 7.75; S, 5.18; Found C, 54.18; H, 4.14; Cl, 5.53; F, 9.38; N, 13.66; O, 7.66; S, 5.12.

*6.1.11.5. Tert-butyl 4-((4-(3-(3-chloro-4 methylphenyl)ureido)phenyl) amino)-5,8 dihydro pyrido [4′,3′:4,5] thieno[2,3-d]pyrimidine-7(6H)-carboxylate **(14e)***. Dark brown crystals. (0.27 g, 53%); m.p > 300 °C. **^{1}H NMR (400 MHz, DMSO-d$_6$)** δ 9.93 (s, 1H, NH D$_2$O exchangeable), 9.85 (s, 2H, NH D$_2$O exchangeable), 8.34 (s, 1H, pyrimidine H), 8.06 (s, 1H, ArH), 7.55 (m, 4H, ArH), 7.26 (d, J = 8 Hz, 1H, ArH), 7.10 (d, J = 8 Hz, 1H, ArH), 3.95 (s, 2H, CH$_2$ pyridine), 3.81 (t, 2H, J = 4 Hz, CH$_2$ pyridine), 2.45 (s, 3H, Ph-CH$_3$), 2.33 (t, 2H, J = 4 Hz, CH$_2$ pyridine), 2.01 (s, 9H, -Boc). **MS**: (Mwt.: 564): m/z, 566 [M$^+$ + 2, (18%)], 564 [M$^+$, (54%)]; **Calcd** for C$_{28}$H$_{29}$ClN$_6$O$_3$S (Mwt.: 564.09) C, 59.51; H, 5.17; Cl, 6.27; N, 14.87; O, 8.49; S, 5.67. Found C, 59.38; H, 5.28; Cl, 6.39; N, 14.78; O, 8.52; S, 5.89.

*6.1.11.6. Tert-butyl 4-((4-(3-phenylthioureido)phenyl)amino)-5,8 dihydro pyrido [4′,3′:4,5] thieno[2,3-d]pyrimidine-7(6H)-carboxylate **(14f)***. Yellowish brown crystals. (0.47 g, 44%); m.p > 300 °C **^{1}H NMR (400 MHz, DMSO-d$_6$)** δ 9.93 (s, 1H, NH D$_2$O exchangeable), 9.85 (s, 2H, NH D$_2$O exchangeable), 8.34 (s, 1H, pyrimidine H), 8.06 (s, 1H, ArH), 7.55 (m, 4H, ArH), 7.26 (d, J = 8 Hz, 1H, ArH), 7.10 (d, J = 8 Hz, 1H, ArH) 3.95 (s, 2H, CH$_2$ pyridine), 3.81 (t, 2H, J = 4 Hz, −CH$_2$ pyridine), 2.33 (t, 2H, J = 4 Hz, CH$_2$ pyridine), 2.01(s, 9H,-Boc). **Calcd** for C$_{27}$H$_{28}$N$_6$O$_2$S$_2$ (Mwt.: 535.17) C, 60.88; H, 5.30; N, 15.78; O, 6.01; S, 12.04. Found C, 60.68; H, 5.22; N, 15.58; O, 6.15; S, 12.22.

*6.1.11.7. Tert-butyl 4-((4-(3-(4-methoxyphenyl)thioureido)phenyl)amino)-5,8-dihydropyrido [4′,3′:4,5]thieno[2,3-d]pyrimidine-7(6H)-carboxylate **(14g)***. Brown crystals. (0.318 g, 63%); m.p > 300 °C. **^{1}H NMR (400 MHz, DMSO-d$_6$)** δ 9.93 (s, 2H, NH D$_2$O exchangeable), 9.83 (s, 1H, NH D$_2$O exchangeable), 8.41(s, 1H, pyrimidine H), 8.38 (d, J = 8 Hz, 1H, ArH), 8.23 (d, J = 8 Hz, 1H, ArH), 8.16 (d, J = 8 Hz, 1H, ArH), 7.63 (d, J = 8 Hz, 1H, ArH), 7.56 (m, 4H, ArH) 4.83 (s, 2H, CH$_2$ pyridine), 4.79 (t, J = 4 Hz, 2H, CH$_2$ pyridine), 3.82 (t, J = 4 Hz, 2H, CH$_2$ pyridine) 3.77 (s, 3H, Ph −OCH$_3$), 1.91 (s, 9H, -Boc). **Calcd** for C$_{28}$H$_{30}$N$_6$O$_3$S$_2$ (Mwt.: 562.18) C, 59.77; H, 5.37; N, 14.94; O, 8.53; S, 11.39. Found C, 59.68; H, 5.22; N, 15.02; O, 6.35; S, 11.52.

*6.1.11.8. Tert-butyl 4-((4-(3-(3,4-dichlorophenyl)ureido)phenyl)amino)-5,8-dihydropyrido [4′,3′:4,5] thieno[2,3-d]pyrimidine-7(6H)-carboxylate **(14h)***. The titled compound was crystallized from ethanol to give brown crystals. (0.24 g, 46%); m.p. > 300 °C **^{1}H NMR (400 MHz, DMSO-d$_6$)** δ 9.94 (s, 1H, NH D$_2$O exchangeable), 9.37 (s, 1H, NH D$_2$O exchangeable), 9.29 (s, 1H, NH D$_2$O exchangeable), 8.40 (s, 1H, pyrimidine H), 8.23 (s, 1H, ArH), 7.65–7.61 (m, 4H, ArH), 7.55 (d, J = 8 Hz, 2H, ArH), 4.78 (s, 2H, CH$_2$ pyridine), 3.83 (t, 2H, J = 4 Hz, CH$_2$ pyridine), 2.79 (t, 2H, J = 4 Hz, CH$_2$ pyridine), 1.91 (s, 9H, -Boc). **Calcd** for C$_{28}$H$_{30}$N$_6$O$_3$S$_2$ (Mwt.: 585.50) C, 55.39; H, 4.48; Cl, 12.11; N, 14.35; O, 8.20; S, 5.48. Found C, 55.19; H, 4.68; Cl, 12.31; N, 14.25; O, 8.36; S, 5.28.

*6.1.11.9. Tert-butyl-4-((4-(3-(4-bromophenyl)ureido)phenyl)amino)-5,8-dihydropyrido [4′,3′:4,5]thieno[2,3-d]pyrimidine-7(6H)-carboxylate **(14i)***. The titled compound was crystallized from methanol as yellowish brown crystals (0.22 g, 42%); m.p. = 280–282 °C **^{1}H NMR (400 MHz, DMSO-d$_6$)** δ 9.93 (s, 1H, NH D$_2$O exchangeable), 8.91 (s, 1H, NH D$_2$O exchangeable), 8.72 (s, 1H, NH D$_2$O exchangeable), 8.37 (s, 1H, pyrimidine H), 7.55 (d, J = 8 Hz, 2H, ArH), 7.49 (d, J = 8 Hz, 2H, ArH), 7.38 (d, J = 8 Hz, 2H, ArH), 7.32 (d, J = 8 Hz, 2H, ArH), 4.77 (s, 2H−CH$_2$ pyridine), 3.81 (t, 2H, J = 4 Hz, CH$_2$ pyridine), 2.15 (t, 2H, J = 4 Hz, CH$_2$-pyridine), 2.04 (s, 9H,-Boc). **MS**: (Mwt.: 595.5): m/z, 597 [M$^+$ + 2, (48%)], 595 [M$^+$, (47.9%)].

Calcd for $C_{27}H_{27}BrN_6O_3S$ (Mwt.: 595.52) C, 54.46; H, 4.57; Br, 13.42; N, 14.11; O, 8.06; S, 5.38. Found C, 54.26; H, 4.65; Br, 13.52; N, 14.32; O, 8.22; S, 5.16.

*6.1.11.10. Tert-butyl 4-((4-(3-(4-methoxyphenyl)ureido)phenyl)amino)-5,8-dihydropyrido [4′,3′:4,5] thieno[2,3-d]pyrimidine-7(6H)-carboxylate **(14j)**.* The titled compound was purified by column chromatography using DCM- EtOAc (8:2) as an eluent and separated as brown crystals (0.2 g, 41%); m.p. > 300 °C **^{1}H NMR (400 MHz, DMSO-d$_6$)** δ 10.04 (s, 2H, NH D_2O exchangeable), 8.73(s, 1H, NH D_2O exchangeable), 8.47 (s, 1H, pyrimidine H), 7.49 (d, J = 8 Hz, 2H, ArH), 7.40 (d, J = 8 Hz, 2H, ArH), 7.34 (d, J = 8 Hz, 2H, ArH), 7.05 (d, J = 8 Hz, 1H, ArH), 6.86 (d, J = 8 Hz, 1H, ArH), 4.45(s, 2H, $\underline{CH_2}$ pyridine), 3.77 (s, 3H, Ph-$\underline{OCH_3}$), 3.06 (t, 2H, J = 4 Hz, $\underline{CH_2}$ pyridine), 2.01 (t, 2H, J = 4 Hz, $\underline{CH_2}$ pyridine), 1.91 (s, 9H, -Boc). **Calcd** for $C_{28}H_{30}N_6O_4S$ (Mwt.: 546.65) C, 61.52; H, 5.53; N, 15.37; O, 11.71; S, 5.86 Found C, 61.29; H, 5.48; N, 15.26; O, 11.68; S, 5.68.

*6.1.11.11. Tert-butyl-4-((4-(3-(4-chlorophenyl)ureido)phenyl)amino)-5,8-dihydropyrido[4′,3′:4,5]thieno[2,3-d]pyrimidine-7(6H)-carboxylate **(14k)**.* The titled compound was separated as brown crystals (0.19 g, 39%); m.p. > 300 °C.**^{1}H NMR (400 MHz, DMSO-d$_6$)** δ 9.93 (s, 1H, NH D_2O exchangeable), 8.91 (s, 1H, NH D_2O exchangeable), 8.72 (s, 1H, NH D_2O exchangeable), 8.37 (s, 1H, pyrimidine H), 7.55 (d, J = 8 Hz, 2H, ArH), 7.50 (d, J = 8 Hz, 2H, ArH), 7.38 (d, J = 8 Hz, 2H, ArH), 7.32 (d, J = 8 Hz, 2H, ArH), 4.77 (s, 2H, $\underline{CH_2}$ pyridine), 3.81 (t, 2H, J = 4 Hz, $\underline{CH_2}$ pyridine), 2.15 (t, 2H, J = 4 Hz, $\underline{CH_2}$ pyridine), 2.04 (s, 9H, -Boc). **^{13}C NMR (100 MHz, DMSO-d$_6$)** δ 169.13, 168.44, 153.21, 139.74, 135.74, 135.051, 134.63, 134.50, 129.02, 128.92, 125.35, 125.24, 124.11, 123.57, 123.49, 123.29, 120.90, 119.95, 119.78, 119.54, 119.41, 80.20, 43.35, 41.58, 24.41, 24.37, 24.31, 22.22. **MS**: (Mwt.: 550): *m/z*, 552 [M^+ + 2, (7.51%)], 550 [M^+, (23.91%)]; **Calcd** for $C_{27}H_{27}ClN_6O_3S$ (Mwt.: 550.01) C, 58.85; H, 4.94; Cl, 6.43; N, 15.25; O, 8.71; S, 5.82 Found C, 58.66; H, 4.73; Cl, 6.32; N, 15.17; O, 8.57; S, 5.64.

6.1.11.12. Tert-butyl-4-((4-(3-(3-fluorophenyl)ureido)phenyl)amino)-5,8-dihydropyrido [4′,3′:4,5]thieno[2,3-d]pyrimidine-7(6H)-carboxylate (14l). Brown crystals. (0.15 g, 30%); m.p > 300 °C. **^{1}H NMR (400 MHz, DMSO-d$_6$)** δ 10.07 (s, 2H, NH D_2O exchangeable), 8.80 (s, 1H, NH D_2O exchangeable), 8.43 (s, 1H, pyrimidine H), 7.74 (d, J = 8 Hz, 2H, ArH), 7.64 (d, J = 8 Hz, 2H, ArH), 7.47 (s, 1H, ArH), 7.40 (d, J = 8 Hz, 2H, ArH) 7.33 (t, J = 8 Hz, 1H, ArH), 4.78 (s, 2H, $\underline{CH_2}$ pyridine), 4.46 (t, J = 4 Hz, 2H, $\underline{CH_2}$ pyridine), 2.15 (t, J = 4 Hz, 2H, $\underline{CH_2}$ pyridine), 1.55 (s, 9H,-Boc). **Calcd** for $C_{27}H_{27}FN_6O_3S$ (Mwt.: 534.06) C, 60.66; H, 5.09; F, 3.55; N, 15.72; O, 8.98; S, 6.00 Found C, 60.47; H, 5.29; F, 3.35; N, 15.66; O, 8.87; S, 6.22.

*6.1.11.13. Tert-butyl-4-((4-(3-(4-fluorophenyl)ureido)phenyl)amino)-5,8-dihydropyrido [4′,3′:4,5]thieno[2,3-d]pyrimidine-7(6H)-carboxylate **(14m)**.* Brown crystals. (0.18 g, 36%); m.p > 300 °C. **^{1}H NMR (400 MHz, DMSO-d$_6$)** δ 9.97 (s, 1H, NH D_2O exchangeable), 9.92 (s, 1H, NH D_2O exchangeable), 9.83 (s, 1H, NH D_2O exchangeable), 8.35 (s, 1H, pyrimidine H), 7.62 (d, J = 8 Hz, 2H, ArH), 7.56 (d, J = 8 Hz, 2H, ArH), 7.09 (m, 4H, ArH), 4.81 (s, 2H, $\underline{CH_2}$ pyridine), 3.95 (t, J = 4 Hz, 2H, $\underline{CH_2}$ pyridine), 3.20 (t, J = 4 Hz, 2H, $\underline{CH_2}$ pyridine), 1.45 (s, 9H, -Boc). **Calcd** for $C_{27}H_{27}FN_6O_3S$ (Mwt.: 534.61) C 60.66; H, 5.09; F, 3.55; N, 15.72; O, 8.98; S, 6.00. Found C, 60.47; H, 5.29; F, 3.35; N, 15.63; O, 8.84; S, 6.18.

*6.1.12. General procedure of preparation of 3-(4-((5,6,7,8-tetrahydropyrido[4′,3′:4,5]thieno[2,3-d]pyrimidin-4-yl)amino)phenyl) 3-substituted 1-Phenylureas and thioureas **15a-m***

General Procedure:

A solution of HCl (4 mL, 4 M) was added dropwise at 0 °C under stirring to a solution of the Boc protected compounds (0.1 gm, 0.2 mmol) **(14a-m)** which were dissolved in suitable solvent such as dioxane or methanol. The homogeneous mixture was stirred for 1–3 h at 0 °C. Reaction completion was judged by TLC in all compounds after 1–3 h. The reaction mixture was condensed under *vacuo* at room temperature. The residue was then washed with diethyl ether and neutralized by 10% aqueous Na_2CO_3. The targeted Compounds **(14a-g)** were further purified by column chromatography using using DCM-EtOAc (9:1) as an eluent in yields 40–75%. Compounds **(15 h-m)** were further purified using column chromatography with DCM:MeOH (9.5:0.5) as an eluent.

*6.1.12.1. 1-Phenyl-3-(4-((5,6,7,8-tetrahydropyrido[4′,3′:4,5]thieno[2,3-d]pyrimidin-4-yl)amino)phenyl)urea **(15a)**.* Light brown crystals. (0.05 g, 63.%); m.p > 300 °C. **^{1}H NMR (400 MHz, DMSO-d$_6$)** δ 9.91 (s, 2H, NH D_2O exchangeable), 9.65 (s, 1H, NH D_2O exchangeable), 8.93 (s, 1H NH D_2O exchangeable), 8.45 (s, 1H, pyrimidine H), 7.73 (t, J = 8 Hz, 1H, ArH), 7.62 (t, J = 8 Hz, 1H, ArH), 7.50 (d, J = 8 Hz, 2H, ArH), 7.39 (d, J = 8 Hz, 2H, ArH), 7.28 (t, J = 8 Hz, 1H, ArH) 7.15 (d, J = 8 Hz, 2H, ArH), 4.47 (s, 2H, $\underline{CH_2}$ pyridine), 2.68 (t, 2H, J = 4 Hz, $\underline{CH_2}$ pyridine), 2.34 (t, 2H, J = 4 Hz, $\underline{CH_2}$ pyridine). **Calcd** for $C_{22}H_{20}N_6O_S$ (Mwt.: 416.50) C, 63.44; H, 4.84; N, 20.18; O, 3.84; S, 7.70 Found C, 63.36; H, 4.72; N, 20.36; O, 3.69; S, 7.59.

*6.1.12.2. 1-(4-((5,6,7,8-Tetrahydropyrido[4′,3′:4,5]thieno[2,3-d]pyrimidin-4-yl)amino)phenyl)-3-(m-tolyl)urea **(15b)**.* Grey crystals. (0.05 g, 71%); m.p > 300 °C.**^{1}H NMR (400 MHz, DMSO-d$_6$)** δ 9.96 (s, 2H, NH D_2O exchangeable), 8.70 (s, 1H, NH D_2O exchangeable), 8.46 (s, 1H, NH D_2O exchangeable) 8.40 (s, 1H, pyrimidine H), 7.72 (d, J = 8 Hz, 2H, ArH), 7.38 (d, J = 8 Hz, 2H, ArH), 7.60 (s, 1H, ArH), 7.27–7.15 (m, 3H, ArH), 4.78 (s, 2H, $\underline{CH_2}$ pyridine), 4.44 (t, 2H, J = 8 Hz, $\underline{CH_2}$ pyridine), 3.10 (t, 2H, J = 8 Hz, $\underline{CH_2}$ pyridine), 2.13 (s, 3H, Ph-$\underline{CH_3}$). **Calcd** for $C_{23}H_{22}N_6OS$ (Mwt.: 430.53) C 64.17; H, 5.15; N, 19.52; O, 3.72; S, 7.45 Found C, 64.37; H, 5.28; N, 19.36; O, 3.66; S, 7.36.

*6.1.12.3. 1-(3-Methoxyphenyl)-3-(4-((5,6,7,8-tetrahydropyrido [4′,3′:4,5]thieno[2,3-d] pyrimidin-4-yl)amino)phenyl)urea **(15c)**.* Buff crystals (0.04 g, 50%); m.p > 300 °C. **^{1}H NMR (400 MHz, DMSO-d$_6$)** δ 9.94 (s, 2H, NH D_2O exchangeable), 9.63 (s, 1H, NH D_2O exchangeable), 8.71 (s, 1H NH D_2O exchangeable of pyridine) 8.47 (s, 1H, pyrimidine H), 7.74 (d, J = 8 Hz, 2H, ArH), 7.49 (d, J = 8 Hz, 2H, ArH), 7.24 (s, 1H, ArH), 6.94 (t, J = 8 Hz, 1H, ArH), 6.58 (d, J = 8 Hz, 2H, ArH), 4.47 (s, 2H, $\underline{CH_2}$ pyridine), 3.71 (t, 2H, J = 4 Hz, $\underline{CH_2}$ pyridine), 3.48 (t, 2H, J = 8 Hz, $\underline{CH_2}$ pyridine), 3.78 (s, 3H, Ph-$\underline{OCH_3}$). **^{13}C NMR (100 MHz, DMSO-d$_6$)** δ 164.65, 164.33, 161.42, 160.33, 155.30, 154.66, 152.96, 140.31, 131.28, 130.05, 125.27, 125.23, 124.28, 123.77, 121.08, 111.04, 108.24, 104.60, 103.04, 55.41, 51.70, 41.97, 22.97. **Calcd** for $C_{23}H_{22}N_6O_2S$ (Mwt.: 446.53) C, 61.87; H, 4.97; N, 18.82; O, 7.17; S, 7.18 Found C, 61.69; H, 4.85; N, 18.62; O, 7.27; S, 7.36.

*6.1.12.4. 1-(4-Chloro-3-(trifluoromethyl)phenyl)-3-(4-((5,6,7,8-tetrahydropyrido [4′,3′:4,5]thieno[2,3-d]pyrimidin-4-yl)amino)phenyl) urea **(15d)**.* The titled compound was separated as brown crystals. (0.04 g, 48%); m.p = 262–264 °C. **^{1}H NMR (400 MHz, DMSO-d$_6$)** δ 9.72 (s, 1H, NH D_2O exchangeable), 9.03 (s, 1H, NH D_2O exchangeable), 8.97 (s, 1H, NH D_2O exchangeable), 8.71 (s, 1H, NH D_2O exchangeable-pyridine), 8.43 (s, 1H, pyrimidine H), 7.47 (d, J = 8 Hz, 1H, ArH), 7.38 (d, J = 8 Hz, 1H, ArH), 7.30 (s, 1H, ArH), 7.07 (d, J = 8 Hz, 2H, ArH) 6.86 (d, J = 8 Hz, 1H, ArH), 6.88 (d, J = 8 Hz, 1H, ArH), 3.86 (s, 2H, -pyridine), 2.66 (t, 2H, J = 4 Hz, -pyridine), 2.31 (t, 2H, J = 4 Hz, -pyridine). **^{13}C NMR (100 MHz, DMSO-d$_6$)** δ 132.44, 129.50, 123.80, 120.34, 113.63, 113.62, 113.58, 113.33, 51.87, 49.06, 23.10. **Calcd** for $C_{23}H_{18}ClF_3N_6OS$ (Mwt.: 518.94) C, 53.23; H, 3.50; Cl, 6.83; F, 10.98; N, 16.19; O, 3.08; S, 6.18 Found C, 53.38; H, 3.39; Cl, 6.76; F, 10.79; N, 16.29; O, 3.26; S, 6.27.

6.1.12.5. 1-(3-Chloro-4-methylphenyl)-3-(4-((5,6,7,8-tetrahydropyrido[4′,3′:4,5]thieno[2,3-d]pyrimidin-4-yl)amino)phenyl)urea ***(15e)***. light brown crystals (0.05 g, 66%); m.p > 300 °C. **^{1}H NMR (400 MHz, DMSO-d$_6$)** δ 10.0 (s, 2H, NH D_2O exchangeable), 9.71 (s, 1H, NH D_2O exchangeable), 8.73 (s, 1H, NH D_2O exchangeable), 8.47 (s, 1H, pyrimidine H), 7.74 (d, J = 8 Hz, 1H, ArH), 7.40 (d, J = 8 Hz, 1H, ArH), 7.29 (s, 1H, ArH), 7.27 (m, 4H, ArH), 4.46 (s, 2H -pyridine), 3.49 (t, 2H, J = 4 Hz, $\underline{CH_2}$ pyridine), 2.35 (t, 2H, J = 4 Hz, $\underline{CH_2}$ pyridine), 2.27 (s, 3H, Ph-$\underline{CH_3}$). **^{13}C NMR (100 MHz, DMSO-d$_6$)** δ 171.70, 166.80, 155.83, 155.66, 142.23, 139.35, 134.14, 132.79, 131.55, 131.36, 130.68, 127.41. 125.51, 125.24, 124.269, 123.79, 123.33, 120.12, 43.40, 42.04, 34.70. **Calcd** for $C_{23}H_{21}ClN_6OS$ (Mwt.: 464.97) C, 59.41; H, 4.55; Cl, 7.62; N, 18.07; O, 3.44; S, 6.90 Found C, 59.22; H, 4.38; Cl, 7.58; N, 18.28; O, 3.24; S, 6.76.

6.1.12.6. 1-Phenyl-3-(4-((5,6,7,8-tetrahydropyrido[4′,3′:4,5]thieno[2,3-d]pyrimidin-4-yl)amino)phenyl)thiourea ***(15f)***. Yellowish brown crystals (0.04 g, 57%); m.p > 300 °C. **^{1}H NMR (400 MHz, DMSO-d$_6$)** δ 9.91 (s, 2H, NH D_2O exchangeable), 9.65 (s, 1H, NH D_2O exchangeable), 8.93 (s, 1H, NH D_2O exchangeable), 8.45 (s, 1H, pyrimidine H), 7.73 (t, J = 8 Hz, 1H, ArH), 7.62 (t, J = 8 Hz, 1H, ArH), 7.50 (d, J = 8 Hz, 2H, ArH), 7.39 (d, J = 8 Hz, 2H, ArH), 7.28 (t, J = 8 Hz, 1H, ArH), 7.15 (d, J = 8 Hz, 2H, ArH), 4.47 (s, 2H, $\underline{CH_2}$-pyridine), 2.68 (t, 2H, J = 4 Hz, $\underline{CH_2}$ pyridine), 2.34 (t, 2H, J = 4 Hz, $\underline{CH_2}$ pyridine). **Calcd** for $C_{22}H_{20}N_6S_2$ (Mwt.: 432.56) C, 61.09; H, 4.66; N, 19.43; S, 14.82 Found C, 61.29; H, 4.48; N, 19.28; S, 14.66.

6.1.12.7. 1-(4-Methoxyphenyl)-3-(4-((5,6,7,8-tetrahydropyrido[4′,3′:4,5]thieno[2,3-d]pyrimidin-4-yl)amino)phenyl)thiourea ***(15g)***. Brown crystals (0.039 g, 48%); m.p > 300 °C. **^{1}H NMR (400 MHz, DMSO-d$_6$)** δ 10.0 (s, 2H, NH D_2O exchangeable), 9.60 (s, 1H, NH D_2O exchangeable), 8.72 (s, 1H, NH D_2O exchangeable), 8.45 (s, 1H, pyrimidine H), 7.73 (d, J = 8 Hz, 2H, ArH), 7.62 (d, J = 8 Hz, 1H, ArH), 7.48 (d, J = 8 Hz, 1H, ArH), 7.39 (d, J = 8 Hz, 2H, ArH), 7.29 (d, J = 8 Hz, 2H, ArH), 4.45 (s, 2H, $\underline{CH_2}$-pyridine), 3.96 (s, 3H, Ph-$\underline{OCH_3}$), 3.11 (t, 2H, J = 4 Hz, $\underline{CH_2}$ pyridine), 2.65 (t, 2H, J = 4 Hz, $\underline{CH_2}$-pyridine). **^{13}C NMR (100 MHz, DMSO-d$_6$)** δ 175.02, 160.55, 159.88, 155.96, 152.65, 134.96, 129.54, 124.27, 123.61, 118.76, 116.25, 115.89, 42.09, 41.24, 34.74, 22.90. **Calcd** for $C_{23}H_{22}N_6OS_2$ (Mwt.: 462.59) C, 59.72; H, 4.79; N, 18.17; O, 3.46; S, 13.86 Found C, 59.66; H, 4.63; N, 18.08; O, 3.28; S, 13.74.

6.1.12.8. 1-(3,4-Dichlorophenyl)-3-(4-((5,6,7,8-tetrahydropyrido[4′,3′:4,5]thieno[2,3-d]pyrimidin-4-yl)amino)phenyl)ureas ***(15h)***. Brown crystals (0.05 g, 62%); m.p > 300 °C. **^{1}H NMR (400 MHz, DMSO-d$_6$)** δ 9.97 (s, 1H, NH D_2O exchangeable), 9.37 (s, 2H, NH D_2O exchangeable),9.29 (s, 1H, NH D_2O exchangeable), 8.40 (s, 1H, pyrimidine H), 8.23 (s, 1H, ArH), 7.61 (s, 4H, ArH), 7.55 (d, J = 8 Hz, 2H, ArH), 4.78 (s, 2H, $\underline{CH_2}$-pyridine) 3.83 (t, 2H, J = 4 Hz, $\underline{CH_2}$ pyridine) 2.79 (t, 2H, J = 4 Hz, $\underline{CH_2}$ pyridine). **Calcd** for $C_{22}H_{18}Cl_2N_6OS$ (Mwt.: 484.06) C, C, 54.44; H, 3.74; Cl, 14.61; N, 17.31; O, 3.30; S, 6.61 Found C, 54.36; H, 3.66; Cl, 14.48; N, 17.21; O, 3.18; S, 6.78.

6.1.12.9. 1-(4-Bromophenyl)-3-(4-((5,6,7,8-tetrahydropyrido[4′,3′:4,5]thieno[2,3-d]pyrimidin-4-yl)amino)phenyl)urea ***(15i)***. Light brown crystals (0.051 g, 63%); m.p > 300 °C. **^{1}H NMR (400 MHz, DMSO-d$_6$)** δ 9.98 (s, 1H, NH D_2O exchangeable), 9.73 (s, 1H, NH D_2O exchangeable), 9.28 (s, 1H, NH D_2O exchangeable),8.72 (s, 1H, NH D_2O exchangeable), 8.45 (s, 1H, pyrimidine H), 7.72 (d, J = 8 Hz, 2H, ArH), 7.47 (d, J = 8 Hz, 2H, ArH), 7.38 (d, J = 8 Hz, 2H, ArH), 7.29 (d, J = 8 Hz, 2H, ArH), 4.44 (s, 2H, $\underline{CH_2}$ pyridine), 3.44 (t, 2H, J = 4 Hz, $\underline{CH_2}$ pyridine), 3.37 (t, 2H, J = 4 Hz, $\underline{CH_2}$ pyridine). **Calcd** for $C_{22}H_{19}BrN_6OS$ (Mwt.: 495.40) C, 53.34; H, 3.87; Br, 16.13; N, 16.96; O, 3.23; S, 6.47 Found C, 53.24; H, 3.67; Br, 16.26; N, 16.78; O, 3.14; S, 6.32.

6.1.12.10. 1-(4-Methoxyphenyl)-3-(4-((5,6,7,8-tetrahydropyrido[4′,3′:4,5]thieno[2,3-d]pyrimidin-4-yl)amino)phenyl)urea ***(15j)***. Buff crystals. (0.036 g, 45%); m.p = 256–258 °C. **^{1}H NMR (400 MHz, DMSO-d$_6$)** δ 10.04 (s, 2H, NH D_2O exchangeable), 9.87 (s, 1H, NH D_2O exchangeable), 8.73 (s, 1H, NH D_2O exchangeable), 8.47 (s, 1H, pyrimidine H), 7.49 (d, J = 8 Hz, 2H, ArH), 7.40 (d, J = 8 Hz, 2H, ArH), 7.34 (d, J = 8 Hz, 2H, ArH), 7.05 (d, J = 8 Hz, 1H, ArH), 6.86 (d, J = 8 Hz, 1H, ArH), 4.45 (s, 2H, $\underline{CH_2}$ pyridine), 3.77 (s, 3H, Ph-$\underline{OCH_3}$), 3.06 (t, 2H, J = 4 Hz, $\underline{CH_2}$ pyridine), 2.01 (t, 2H, J = 4 Hz, $\underline{CH_2}$ pyridine). **Calcd** for $C_{23}H_{22}N_6O_2S$ (Mwt.: 446.15) C, 61.87; H, 4.97; N, 18.82; O, 7.17; S, 7.18 Found C, 61.69; H, 4.76; N, 18.74; O, 7.29; S, 7.32.

6.1.12.11. 1-(4-Chlorophenyl)-3-(4-((5,6,7,8-tetrahydropyrido[4′,3′:4,5]thieno[2,3-d]pyrimidin-4-yl)amino)phenyl)urea ***(15k)***. Golden brown crystals. (0.03 g, 58%); m.p = 298–300 °C. **^{1}H NMR (400 MHz, DMSO-d$_6$)** δ 9.98 (s, 1H, NH D_2O exchangeable), 9.73 (s, 1H, NH D_2O exchangeable), 9.28 (s, 1H, NH D_2O exchangeable),8.72 (s, 1H, NH D_2O exchangeable), 8.45 (s, 1H, pyrimidine H), 7.72 (d, J = 8 Hz, 2H, ArH), 7.47 (d, J = 8 Hz, 2H, ArH), 7.38 (d, J = 8 Hz, 2H, ArH), 7.29 (d, J = 8 Hz, 2H, ArH), 4.44 (s, 2H, $\underline{CH_2}$ pyridine), 3.44 (t, J = 4, 2H, $\underline{CH_2}$ pyridine), 3.37 (t, J = 8 Hz, 2H, $\underline{CH_2}$ pyridine). **^{13}C NMR (100 MHz, DMSO-d$_6$)** δ 155.75, 153.19, 139.48, 138.94, 138.58, 130.03, 129.01, 125.61, 125.33, 124.21, 123.81, 119.77, 119.27, 116.31, 72.77, 70.43, 69.95, 63.21, 60.48, 41.82, 34.67, 22.97. **MS**: (Mwt.: 450): *m/z*, 452 [M^+ + 2, (5%)], 450 [M^+, (15%)]; **Calcd** for $C_{22}H_{19}ClN_6OS$ (Mwt.: 450.95) C, 58.60; H, 4.25; Cl, 7.86; N, 18.64; O, 3.55; S, 7.11 Found C, 58.72; H, 4.38; Cl, 7.98; N, 18.58; O, 3.48; S, 7.38.

6.1.12.12. 1-(3-Fluorophenyl)-3-(4-((5,6,7,8-tetrahydropyrido[4′,3′:4,5]thieno[2,3-d]pyrimidin-4-yl)amino)phenyl)urea ***(15l)***. Brown crystals. (0.032 g, 41%); mp > 300 °C. **^{1}H NMR (400 MHz, DMSO-d$_6$)** δ 10.3 (s, 1H, NH D_2O exchangeable), 10.07 (s, 2H, NH D_2O exchangeable), 8.80 (s, 1H, NH D_2O exchangeable), 8.43 (s, 1H, pyrimidine H), 7.74 (d, J = 8 Hz, 2H, ArH), 7.64 (d, J = 8 Hz, 2H, ArH), 7.47 (s, 1H, ArH), 7.40 (d, J = 8 Hz, 2H, ArH) 7.33 (t, J = 8 Hz, 1H, ArH), 4.78 (s, 2H, $\underline{CH_2}$ pyridine), 4.46(t, J = 4 Hz, 2H, $\underline{CH_2}$ pyridine), 2.15 (t, J = 4 Hz, 2H, $\underline{CH_2}$ pyridine). **Calcd** for $C_{22}H_{19}FN_6OS$ (Mwt.: 434.49) C, 60.82; H, 4.41; F, 4.37; N, 19.34; O, 3.68; S, 7.38 Found C, 60.68; H, 4.29; F, 4.19; N, 19.28; O, 3.56; S, 7.31.

6.1.12.13. 1-(4-Fluorophenyl)-3-(4-((5,6,7,8-tetrahydropyrido[4′,3′:4,5]thieno[2,3-d]pyrimidin-4-yl)amino)phenyl)urea ***(15m)***. Yellowish brown crystals. (0.05 g, 64%); mp > 300 °C. **^{1}H NMR (400 MHz, DMSO-d$_6$)** δ 9.97 (s, 2H, NH D_2O exchangeable), 9.92 (s, 1H, NH D_2O exchangeable), 9.83 (s, 1H, NH D_2O exchangeable), 8.35 (s, 1H, pyrimidine H), 7.60 (d, J = 8 Hz, 2H, ArH), 7.56 (d, J = 8 Hz, 2H, ArH), 7.12–7.09 (m, 4H, ArH), 4.81 (s, 2H, $\underline{CH_2}$ pyridine), 3.95 (t, J = 4 Hz, 2H, $\underline{CH_2}$ pyridine), 3.20 (t, J = 4 Hz, 2H, $\underline{CH_2}$ pyridine). **MS**: (Mwt.: 434.4): *m/z*, 434 [M^+, (15.2%)] **Calcd** for $C_{22}H_{19}ClN_6OS$ (Mwt.: 434.49) C, 60.82; H, 4.41; F, 4.37; N, 19.34; O, 3.68; S, 7.38 Found C, 60.65; H, 4.26; F, 4.23; N, 19.16; O, 3.57; S, 7.29.

Acknowledgement

The authors are very thankful to Bpsbioscience, San Diego, USA, for Kinase assays on all of the synthesized compounds. Also many thanks to Future University in Egypt for financial assistance in this research. We are very grateful to both Vacsera, Chemotherapeutic Research section, Egypt, for performing the cell cycle and caspase-3 assays and to the 'NCI' Bethesda, Maryland for the *in vitro* Antiproliferative screening of the compounds against 60 cell line panel. The authors declare no competing financial interests and have no other affiliations. No any writing assistance was used in the writing of this manuscript.

Appendix A. Supplementary material

Supplementary data to this article can be found online at https://doi.org/10.1016/j.bioorg.2018.10.008.

References

[1] E.M. Bridges, A.L. Harris, The angiogenic process as a therapeutic target in cancer, Biochem. Pharmacol. 81 (10) (2011) 1183–1191.
[2] J. Folkman, Opinion: angiogenesis: an organizing principle for drug discovery? Nat. Rev. Drug Discov. 6 (4) (2007) 273.
[3] P. Carmeliet, Angiogenesis in life, disease and medicine, Nature 438 (7070) (2005) 932.
[4] J. Folkman (Ed.), Role of Angiogenesis in Tumor Growth and Metastasis, Semin Oncol. Elsevier, 2002.
[5] Y. Liu, N.S. Gray, Rational design of inhibitors that bind to inactive kinase conformations, Nat. Chem. Biol. 2 (7) (2006) 358.
[6] J. Blanc, R. Geney, C. Menet, Type II kinase inhibitors: an opportunity in cancer for rational design, Anti-Cancer Agents in Med. Chem. (Formerly Current Medicinal Chemistry-Anti-Cancer Agents) 13 (5) (2013) 731–747.
[7] Q.-Q. Xie, H.-Z. Xie, J.-X. Ren, L.-L. Li, S.-Y. Yang, Pharmacophore modeling studies of type I and type II kinase inhibitors of Tie2, J. Mol. Graph. Model. 27 (6) (2009) 751–758.
[8] L.M. Strawn, G. McMahon, H. App, R. Schreck, W.R. Kuchler, M.P. Longhi, T.H. Hui, C. Tang, A. Levitzki, A. Gazit, Flk-1 as a target for tumor growth inhibition, Cancer Res. 56 (15) (1996) 3540–3545.
[9] V.A. Machado, D. Peixoto, R. Costa, H.J. Froufe, R.C. Calhelha, R.M. Abreu, I.C. Ferreira, R. Soares, M.-J.R. Queiroz, Synthesis, antiangiogenesis evaluation and molecular docking studies of 1-aryl-3-[(thieno [3, 2-b] pyridin-7-ylthio) phenyl] ureas: discovery of a new substitution pattern for type II VEGFR-2 Tyr kinase inhibitors, Biorg. Med. Chem. 23 (19) (2015) 6497–6509.
[10] A. Ghith, N.S. Ismail, K. Youssef, K.A. Abouzid, Medicinal attributes of thienopyrimidine based scaffold targeting tyrosine kinases and their potential anticancer activities, Arch. Pharm. 350 (11) (2017).
[11] A.E. Rashad, A.H. Shamroukh, R.E. Abdel-Megeid, W.A. El-Sayed, Synthesis, reactions, and antimicrobial evaluation of some polycondensed thienopyrimidine derivatives, Synth. Commun. 40 (8) (2010) 1149–1160.
[12] A.E. Rashad, A.H. Shamroukh, H.H. Sayed, S.M. Awad, N.A. Abdelwahed, Some novel thiopyrimidine nucleoside analogs: synthesis and in vitro antimicrobial evaluation, Synth. Commun. 41 (5) (2011) 652–661.
[13] V.S. Dinakaran, B. Bomma, K.K. Srinivasan, Fused pyrimidines: the heterocycle of diverse biological and pharmacological significance, Der. Pharma Chem. 4 (1) (2012) 255–265.
[14] J. Ding, X. Chen, Z. Gao, X. Dai, L. Li, C. Xie, H. Jiang, L. Zhang, D. Zhong, Metabolism and pharmacokinetics of novel selective vascular endothelial growth factor receptor-2 inhibitor apatinib in humans, Drug Metab. Dispos. (2013) dmd. 112.050310.
[15] Y. Oguro, N. Miyamoto, K. Okada, T. Takagi, H. Iwata, Y. Awazu, H. Miki, A. Hori, K. Kamiyama, S. Imamura, Design, synthesis, and evaluation of 5-methyl-4-phenoxy-5H-pyrrolo [3, 2-d] pyrimidine derivatives: novel VEGFR2 kinase inhibitors binding to inactive kinase conformation, Biorg. Med. Chem. 18 (20) (2010) 7260–7273.
[16] M.A. Aziz, R.A. Serya, D.S. Lasheen, A.K. Abdel-Aziz, A. Esmat, A.M. Mansour, A.N.B. Singab, K.A. Abouzid, Discovery of potent VEGFR-2 inhibitors based on furopyrimidine and thienopyrimidne scaffolds as cancer targeting agents, Sci. Rep. 6 (2016) 24460.
[17] K. Okamoto, M. Ikemori-Kawada, A. Jestel, K. von König, Y. Funahashi, T. Matsushima, A. Tsuruoka, A. Inoue, J. Matsui, Distinct binding mode of multikinase inhibitor lenvatinib revealed by biochemical characterization, ACS Med. Chem. Lett. 6 (1) (2014) 89–94.
[18] P.A. Harris, A. Boloor, M. Cheung, R. Kumar, R.M. Crosby, R.G. Davis-Ward, A.H. Epperly, K.W. Hinkle, R.N. Hunter III, J.H. Johnson, Discovery of 5-[[4-[(2, 3-dimethyl-2 H-indazol-6-yl) methylamino]-2-pyrimidinyl] amino]-2-methyl-benzenesulfonamide (Pazopanib), a novel and potent vascular endothelial growth factor receptor inhibitor, J. Med. Chem. 51 (15) (2008) 4632–4640.
[19] J.R. Simard, M.u. Getlik, C. Grütter, V. Pawar, S. Wulfert, M. Rabiller, D. Rauh, Development of a fluorescent-tagged kinase assay system for the detection and characterization of allosteric kinase inhibitors, J. Am. Chem. Soc. 131 (37) (2009) 13286–13296.
[20] M. McTigue, B.W. Murray, J.H. Chen, Y.-L. Deng, J. Solowiej, R.S. Kania, Molecular conformations, interactions, and properties associated with drug efficiency and clinical performance among VEGFR TK inhibitors, Proc. Natl. Acad. Sci. 109 (45) (2012) 18281–18289.
[21] Y. Dai, K. Hartandi, Z. Ji, A.A. Ahmed, D.H. Albert, J.L. Bauch, J.J. Bouska, P.F. Bousquet, G.A. Cunha, K.B. Glaser, Discovery of N-(4-(3-Amino-1 H-indazol-4-yl) phenyl)-N' -(2-fluoro-5-methylphenyl) urea (ABT-869), a 3-aminoindazole-based orally active multitargeted receptor tyrosine kinase inhibitor, J. Med. Chem. 50 (7) (2007) 1584–1597.
[22] F. Rodríguez, I. Rozas, M. Kaiser, R. Brun, B. Nguyen, W.D. Wilson, R.N. García, C. Dardonville, New bis (2-aminoimidazoline) and bisguanidine DNA minor groove binders with potent in vivo antitrypanosomal and antiplasmodial activity, J. Med. Chem. 51 (4) (2008) 909–923.
[23] W.M. Eldehna, S.M. Abou-Seri, A.M. El Kerdawy, R.R. Ayyad, A.M. Hamdy, H.A. Ghabbour, M.M. Ali, D.A.A. El Ella, Increasing the binding affinity of VEGFR-2 inhibitors by extending their hydrophobic interaction with the active site: design, synthesis and biological evaluation of 1-substituted-4-(4-methoxybenzyl) phthalazine derivatives, Eur. J. Med. Chem. 113 (2016) 50–62.
[24] E.S. Fondjo, D. Döpp, G. Henkel, Reactions of some anellated 2-aminothiophenes with electron poor acetylenes, Tetrahedron 62 (29) (2006) 7121–7131.
[25] F.D. Bellamy, K. Ou, Selective reduction of aromatic nitro compounds with stannous chloride in non acidic and non aqueous medium, Tetrahedr. Lett. 25 (8) (1984) 839–842.
[26] Y. Han, K. Ebinger, L.E. Vandevier, J.W. Maloney, D.S. Nirschl, H.N. Weller, Efficient and library-friendly synthesis of furo-and thieno [2, 3-d] pyrimidin-4-amine derivatives by microwave irradiation, Tetrahedr. Lett. 51 (4) (2010) 629–632.
[27] C. Wu, M. Wang, Q. Tang, R. Luo, L. Chen, P. Zheng, W. Zhu, Design, synthesis, activity and docking study of sorafenib analogs bearing sulfonylurea unit, Molecules 20 (10) (2015) 19361–19371.
[28] T. Kaiya, T. Fujiwara, K. Kohda, Syntheses and properties of 1-methyl-3-phenylaminobenzimidazolium salts, models of DNA adducts of N7-arylaminodeoxyguanosinium salt, Chem. Res. Toxicol. 13 (10) (2000) 993–1001.
[29] I. Rusznák, J. Bozzay, Á. Dávid, É. Gabriella, On the solubility of pesticides and compounds of pesticide type, Period. Polytech. Chem. Eng. 23 (2) (1979) 87.
[30] R. Arora, S. Paul, R. Gupta, A mild and efficient procedure for the conversion of aromatic carboxylic esters to secondary amides, Can. J. Chem. 83 (8) (2005) 1137–1140.
[31] Y.f. Ji, H. Yan, Q.b. Jiang, Effective nitration of anilides and acrylamides by tert-butyl nitrite, Eur. J. Org. Chem. 2015 (9) (2015) 2051–2060.
[32] I. Havelange, 5 Organisation et institutions scolaires, Histoire de l'éducation. 79 (1) (1998) 110–170.
[33] S. Sayyah, I. Sabbah, F. Said, Characterization and radiometric studies on poly (methyl methacrylate) doped with some amine derivatives, Acta Polym. 40 (8) (1989) 516–520.
[34] Y. Zhu, T. Ran, X. Chen, J. Niu, S. Zhao, T. Lu, W. Tang, Synthesis and biological evaluation of 1-(2-Aminophenyl)-3-arylurea derivatives as potential EphA2 and HDAC dual inhibitors, Chem. Pharm. Bull. 64 (8) (2016) 1136–1141.
[35] S. Karra, Y. Xiao, X. Chen, L. Liu-Bujalski, B. Huck, A. Sutton, A. Goutopoulos, B. Askew, K. Josephson, X. Jiang, SAR and evaluation of novel 5H-benzo [c][1, 8] naphthyridin-6-one analogs as Aurora kinase inhibitors, Bioorg. Med. Chem. Lett. 23 (10) (2013) 3081–3087.
[36] L.S. Reddy, S.K. Chandran, S. George, N.J. Babu, A. Nangia, Crystal structures of N-Aryl-N′-4-nitrophenyl ureas: molecular conformation and weak interactions direct the strong hydrogen bond synthon, Cryst. Growth Des. 7 (12) (2007) 2675–2690.
[37] L.-L. Yang, G.-B. Li, S. Ma, C. Zou, S. Zhou, Q.-Z. Sun, C. Cheng, X. Chen, L.-J. Wang, S. Feng, Structure–activity relationship studies of pyrazolo [3, 4-d] pyrimidine derivatives leading to the discovery of a novel multikinase inhibitor that potently inhibits FLT3 and VEGFR2 and evaluation of its activity against acute myeloid leukemia in vitro and in vivo, J. Med. Chem. 56 (4) (2013) 1641–1655.
[38] Z. Cui, X. Li, L. Li, B. Zhang, C. Gao, Y. Chen, C. Tan, H. Liu, W. Xie, T. Yang, Design, synthesis and evaluation of acridine derivatives as multi-target Src and MEK kinase inhibitors for anti-tumor treatment, Biorg. Med. Chem. 24 (2) (2016) 261–269.
[39] M. Uno, H.S. Ban, W. Nabeyama, H. Nakamura, de novo Design and synthesis of N-benzylanilines as new candidates for VEGFR tyrosine kinase inhibitors, Org. Biomol. Chem. 6 (6) (2008) 979–981.
[40] B. Zhang, Y. Zhao, X. Zhai, L. Wang, J. Yang, Z. Tan, P. Gong, Design, synthesis and anticancer activities of diaryl urea derivatives bearing N-acylhydrazone moiety, Chem. Pharm. Bull. 60 (8) (2012) 1046–1054.
[41] V. Štrukil, D. Margetić, M.D. Igrc, M. Eckert-Maksić, T. Friščić, Desymmetrisation of aromatic diamines and synthesis of non-symmetrical thiourea derivatives by click-mechanochemistry, Chem. Commun. 48 (78) (2012) 9705–9707.
[42] A. Fahmy, S. Esawy, Acid azides Part 2, reactions of acid azides with hydrazides, amines and amino acids, ChemInform. 5 (6) (1974).
[43] B. Yu, Y.-L. Li, S.-H. Song, X.-L. Ji, M.-S. Lin, C.-F. Wu, Design, synthesis and antitumor activity of 4-aminoquinazoline derivatives targeting VEGFR-2 tyrosine kinase, Bioorg. Med. Chem. Lett. 22 (1) (2012) 110–114.
[44] M.S. Abaee, S. Cheraghi, Efficient three-component Gewald reactions under Et3N/H2O conditions, J. Sulfur Chem. 35 (3) (2014) 261–269.
[45] M. Hrast, S. Turk, I. Sosič, D. Knez, C.P. Randall, H. Barreteau, C. Contreras-Martel, A. Dessen, A.J. O'Neill, D. Mengin-Lecreulx, Structure–activity relationships of new cyanothiophene inhibitors of the essential peptidoglycan biosynthesis enzyme MurF, Eur. J. Med. Chem. 66 (2013) 32–45.
[46] J.-J. Dai, C. Fang, B. Xiao, J. Yi, J. Xu, Z.-J. Liu, X. Lu, L. Liu, Y. Fu, Copper-promoted Sandmeyer trifluoromethylation reaction, J. Am. Chem. Soc. 135 (23) (2013) 8436–8439.